REVIEW

Check for updates

Magnetically anisotropic hydrogels for tissue engineering

Lili Hao and Hongli Mao 🄳 *

Many soft tissues of the human body possess hierarchically anisotropic structures, exhibiting orientation-specific mechanical properties and biological functionality. Hydrogels have been proposed as promising scaffold materials for tissue engineering applications due to their water-rich composition, excellent biocompatibility, and tunable physico-chemical properties. However, conventional hydrogels with homogeneous structures often exhibit isotropic properties that differ from those of biological tissues, limiting their further application. Recently, magnetically anisotropic hydrogels containing long-range ordered magneto-structures have attracted widespread interest owing to their highly controllable assembly strategy, rapid magnetic responsiveness and remote spatiotemporal regulation. In this review, we summarize the latest progress of magnetically anisotropic hydrogels for tissue engineering. The fabrication strategy of magnetically anisotropic hydrogels from magnetic nanofillers with different dimensions is systemically introduced. Then, the effects of magnetically anisotropic cues on the physicochemical properties of hydrogels and the cellular biological behavior are discussed. And the applications of magnetically anisotropic hydrogels in the engineering of different tissues are emphasized. Finally, the current challenges and the future perspectives for magnetically anisotropic hydrogels are presented.

1. Introduction

Tissue engineering aims at recreating tissue to repair defects *in vivo*, while accelerating wound healing and reducing medical complications.[1,2] Therefore, tissue-engineered biomimetic scaffolds should have a structure and composition that mimic the extracellular matrix to provide cells with a wide range of biochemical and biophysical cues. The natural extracellular matrix (ECM) contains fibrous structural proteins for maintaining structure, adhesive proteins for signaling, and non-structural proteins for storing bioactive substances, which play important roles in cellular transport properties, mechanical transduction, and growth factor signal transduction.[3–5] Furthermore, many biological tissues, such as skeletal muscle, bone, and cartilage, exhibit anisotropic properties derived from inherent ordered structures and are crucial for maintaining physiological activities and adapting to complex environments.[6–8] For example, skeletal muscle, as the core of our driving system, self-assembles its collagen proteins into 1D fiber bundles that orient and aggregate under the action of motor proteins, generating directed forces or providing shock absorption.[9,10] Similarly, the ordered multilayered structure

composed of collagen fibers provides cartilage with a mechanism for low friction, high strength, and energy dissipation.[11] Thus, biomimetic scaffolds replicating the multilevel ordered hierarchy is also of great importance for tissue repair and functional recovery.

Among the many biomaterials, hydrogels with water-swollen 3D network structures are among the most promising candidates for the development of tissue engineering biomimetic scaffolds, which is mainly owing to their water-rich composition similar to the native ECM, excellent biocompatibility, elasticity, thixotropy, and ease of functionalization.[12–16] Based on the different sources of raw materials, hydrogels can be classified into natural polymer hydrogels (such as gelatin, sodium alginate, hyaluronic acid, silk fibroin, and chitosan) and synthetic polymer hydrogels (such as polyacrylic acid, polyvinyl alcohol, and polyacrylamide), and the appropriate hydrogel type can be selected according to specific application requirements.[17–20] Moreover, the chemical and biophysical properties of the obtained hydrogels can be efficiently modulated by changing the way and degree of crosslinking.[21–24] However, the isotropic nature of conventional hydrogels limits their potential to mimic the anisotropic features of different biological tissues *in vivo*.[25–27] To fabricate structurally anisotropic hydrogels, many methods have been developed to induce a particular orientation of nanofillers or fibrous networks, including electric/magnetic field-induced self-assembly,[28,29] mechanical stretching,[30] electrospinning,[31]

Research Institute for Biomaterials, Tech Institute for Advanced Materials, College of Materials Science and Engineering, Nanjing Tech University, Nanjing 211816, China. E-mail: h.mao@njtech.edu.cn

directional freeze-casting,[32] shear stress-induced alignment,[33] *etc*. But many approaches have their own limitations. For example, the electric field approach strongly relies on the electrochemical stability of hydrogels; the mechanical stretching approach demands a tough hydrogel precursor; the electrospinning approach cannot control the interval between deposited fibers very well; the directional freeze-casting approach faces challenges in precisely controlling the thermal gradient; the shear alignment approach exhibits a decreased performance when faced with thick scaffolds.[2,34,35] By contrast, employing magnetic fields to fabricate anisotropic hydrogels has attracted intensive research, because the space-pervasive nature of magnetic fields makes their applications nondestructive, noncontact, remotely controllable and fully biocompatible.[36,37] With the application of an external magnetic field, the magnetic nanofillers will form long-range ordered structures in the 3D network of nanocomposite hydrogels, achieving a controlled design of magnetically anisotropic biomimetic scaffolds.[2,7] Magneto-responsive hydrogels with an anisotropic structure usually exhibit significant anisotropic mechanical properties similar to the ECM, an enhanced magnetocaloric effect and conductivity.[38,39] Furthermore, magnetically anisotropic hydrogels combined with on-demand magnetic stimuli generated from applied magnetic fields can provide cells with a specific ordered structure and regulate their biological behavior, recreating the architectures of native tissues.[40–42]

Due to the unique advantages and application value of magnetic hydrogels, there have been several excellent reviews that have summarized their fabrication strategies, physicochemical properties, and biomedical applications.[21,43–46] However, relatively less attention has been paid to magnetic hydrogels with anisotropic structures, despite their bright prospects in the field of tissue engineering. Therefore, a comprehensive review that covers the design strategy, anisotropic properties, novel functionality and specific applications in tissue engineering of magnetic hydrogels with an ordered structure is essential and meaningful. In this review, we aim to summarize the significant advances in magneto-responsive hydrogels with an anisotropic structure in tissue engineering, mainly focusing on the fabrication strategies of magnetically anisotropic hydrogels from magnetic nanomaterials with different dimensions (0D, 1D, 2D). We also highlight the versatility of magnetically anisotropic hydrogels, including the enhanced or regulatory effect of magnetically anisotropic cues on hydrogels' mechanical, thermal and optical/electrical properties as well as cell behavior. Moreover, the applications of recently reported magnetically anisotropic hydrogels in various tissue engineering fields (such as skeletal muscle, cartilage, tendon and nerve tissue engineering) are discussed. Finally, the future development and prospects for magnetically anisotropic hydrogels are discussed to improve their application potential in different biomedical fields (Scheme 1).
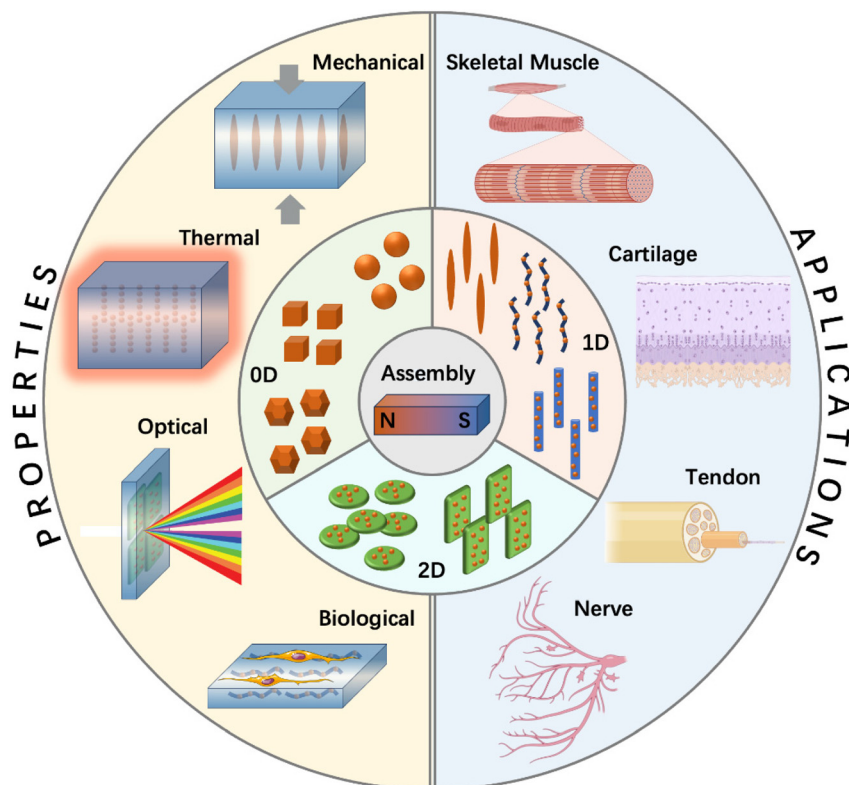
Scheme 1 Schematic illustrations of the fabrication, properties and tissue engineering applications of magnetically anisotropic hydrogels.

2. Fabrication strategies of magnetically anisotropic hydrogels

Hydrogels with magnetic components embedded in the matrix network are generally referred to as magnetic hydrogels.[47] The properties of magnetic hydrogels (*e.g.* magnetic responsiveness and mechanical stability) depend not only on the type of hydrogel and magnetic materials, but also on the concentration, size, morphology and distribution of the magnetic materials as well as the interactions between magnetic materials and the polymer networks.[48] Several common approaches have been developed to fabricate magnetic hydrogels, including the blending method, *in situ* precipitation method and grafting-onto method, which has been described in detail in previous reviews.[43,45] Many biological soft tissues exhibit well-defined structural anisotropy, which is closely related to their orientation-specific performance and physiological activities.[2] Therefore, the introduction of ordered structures in magnetic hydrogels to simulate the structure and properties of anisotropic tissues and provide suitable microenvironments for cells is of great significance to promote their application in tissue engineering. Based on the intrinsic properties of magnetic nanomaterials, magnetically anisotropic hydrogels can be effectively prepared by magneto-induced self-assembly technology.[21] With the application of an external magnetic field, magnetic nanomaterials are magnetized due to the existence of magnetically responsive electrons in the objects, thus forming long-range ordered structures in polymer network matrixes.[49] The ordered structures of magnetic hydrogels can be modulated systematically by changing the size and concentration of magnetic materials and the characteristics of the applied magnetic field.[50] In the process of hydrogel gels, this anisotropic structure can be well fixed in the hydrogel network. This magneto-induced self-assembly strategy has become the most common and popular approach for preparing magnetically anisotropic hydrogels because it has no restrictions on the dimension of the magnetic materials and the orientation direction of hydrogel samples.[7] In this section, we present recent progress in magneto-induced self-assembly within hydrogel matrices based on the ordered arrangement of magnetic nanofillers, including 0D, 1D, and 2D magnetic nanomaterials (Table 1).

## 2.1 Self-assembly of 0D magnetic nanomaterials

Due to their rapid and reversible magnetic responsiveness, magnetic nanoparticles (MNPs) have been extensively investigated as response nanounits to construct magnetically anisotropic hydrogels.[51,52] Under magnetic dipole interactions, MNPs inside hydrogel precursor solutions tend to rapidly form long-range chain or columnar structures parallel to the direction of the external magnetic field.[50,53] Among various magnetic nanomaterials, iron oxide-based MNPs (*e.g.* γ-Fe_2O_3 and Fe_3O_4) have become the most potential candidates for tissue engineering due to their excellent biocompatibility, good chemical stability, easy functionalization and high sensitivity to the application of external magnetic stimuli.[50] Moreover, iron oxide-based MNPs with high saturation magnetization can be induced to align using a low-intensity magnetic field, thereby avoiding the potential risks caused by the use of high-intensity magnetic fields.[21]

Based on the efficient self-assembly behavior of MNPs, a variety of magnetically anisotropic hydrogels have been developed for use in different biological fields. Hu *et al.*[38] reported a novel magneto-response hydrogel with an anisotropic align-

Table 1 Different strategies for fabricating magnetically anisotropic hydrogels

Nano-objects	Magnetic core	Hydrogel matrix	Magnetic field	Properties and application	Ref.
0D	IO NPs	GelMA	0.02 T	C2C12 skeletal myoblasts differentiate toward myotubes Soft robotics	55
	MNPs	Collagen	255 G	Neuronal growth in the direction of the magnetically aligned cues	54
	$Fe_3O_4@SiO_2$ NPs	Polyacrylamide	80 mT	Enhanced magnetothermal effect and controlled drug release	38
	Streptavidin-coated MNPs	Agarose, collagen	2 mT	Cartilage tissue engineering	72
1D	$Fe_3O_4@SiO_2$ NRs	GelMA	7.5 mT	Regulation of the differentiation of iPSCs	59
	IO NRs	Polyisocyanide	20 mT	Anisotropic mechanical properties	36
	Rod-shape magnetic CNC	Gelatin	108 mT	Induction of the directional growth of hASCs	56
	PLGA-based magnetic fibers	Fibrin	100 mT	Stimulation of fibroblasts and functional nerve cells to grow in a linear manner.	65
	Rod-shaped magnetic microgels	Star-PEG-OH	100 mT	Triggering of the alignment of fibroblasts and nerve cells in 3D	37
	MSNFs	GelMA	80 mT	Skeletal muscle regeneration	73
	CNCs	Polyacrylamide	9.4 T	Diffraction gratings	74
2D	MoS_2/Fe_3O_4 NSs	PNIPAm	1 T	Modulation of the photothermal efficiency and the optical properties	58
	Fe/Al_2O_3 platelets	*N*-isopropylacrylamide	300 mT	Multidimensional intelligent anticounterfeiting	66
	TiNS	Poly(vinyl alcohol)	10 T	Optical and mechanical anisotropies	75

IO: iron oxide, MNPs: magnetic nanoparticles, NRs: nanorods, NSs: nanosheets, CNC: cellulose nanocrystal, GelMA: gelatin methacrylate, iPSCs: human induced pluripotent stem cells, hASCs: human adipose-derived stem cells, Star-PEG-OH: six-armed star-shaped poly(ethylene oxide-stat-propylene oxide), MSNFs: magnetic controlled short nanofibers, PNIPAm: poly(*N*-isopropyl acrylamide).
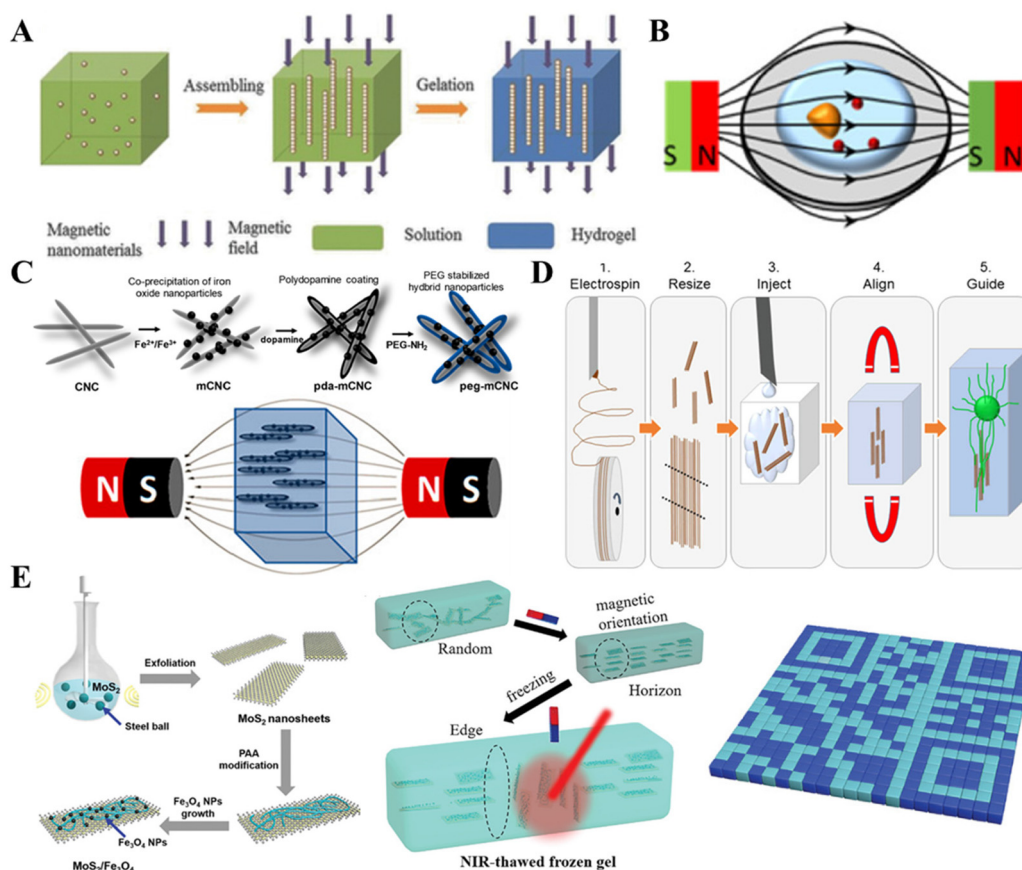
Fig. 1 (A) Schematic illustration of the fabrication process of magnetically anisotropic hydrogels based on 0D nanomaterials.[38] (Reprinted with permission from Wiley, copyright 2015.) (B) Schematic overview of the particle alignment induced by magnetic actuation.[54] (Reprinted with permission from American Chemical Society, copyright 2016.) (C) Schematic representation of the nanoparticle synthesis and the 1D nanomaterial alignment in the hydrogels.[56] (Reprinted with permission from American Chemical Society, copyright 2019.) (D) Schematic diagram of the fabrication process of magnetically anisotropic hydrogels based on 1D nanomaterials prepared by electrospinning.[57] (Reprinted with permission from American Chemical Society, copyright 2019.) (E) Schematic illustration of the synthesis process of MoS_2/Fe_3O_4 and programming the orientation of magnetic nanosheets under a magnetic field, followed by NIR light-treatment of frozen hydrogels. Fluorescent quick dot-matrix response (QR) codes based on PNIPAm-MoS_2/Fe_3O_4 hydrogels.[58] (Reprinted with permission from Wiley, copyright 2022.)

ment of magnetic colloids inside for drug delivery. The mixture solution containing magnetic nanospheres was poured into the module that was exposed to a static magnetic field, with the field lines perpendicular to the horizontal plane (Fig. 1A). The solution was then heated to 50 °C to trigger the gelation of polyacrylamide, thereby stabilizing the assembled structures. Antman-Passig *et al.*[54] developed a new approach to dynamically and remotely control the alignment of magnetic gels *in situ*. With the application of an external magnetic field, the MNPs aggregated into magnetic strings, resulting in the arrangement of the collagen fibers (Fig. 1B). In another work, Tognato *et al.*[55] prepared polyethylene glycol-capped MNPs through co-precipitation and solvothermal methods, and then mixed them into methacryloyl gelatin (GelMA) solution to obtain a homogeneous suspension by vortexing. After that, the solution was immersed in a 0.02 Tesla magnetostatic field generated by two NdFeB permanent magnetic configurations, triggering the MNPs to assemble in oriented filaments along the magnetic flux (Fig. 2A). The 1D assembly struc-

tures obtained served as supportive cues to promote the formation of an elongated co-oriented morphology in neurons.

2.2 Self-assembly of 1D magnetic nanomaterials

Research has shown that magnetically anisotropic hydrogels constructed by the incorporation of 0D MNPs still have certain limitations in the expected applications, because the aggregation and interaction between individual MNPs under magnetic fields are not easy to control.[21] As alternatives, 1D magnetic nanomaterials (*e.g.* nanorods and nanowires) have attracted attention owing to their unique properties. They are aligned rapidly within the hydrogels along the magnetic axis to reconstruct the hierarchically ordered composite structures of natural tissues.[7] For example, Goodrich *et al.*[59] synthesized $Fe_3O_4@SiO_2$ nanorods using a hydrothermal method and utilized multiple electromagnetic magnets to construct an anisotropic complex magnetic field (7.5 mT) to induce the arrangement of the magnetic nanorods (MNRs) (Fig. 2B). This strategy not only enhances the
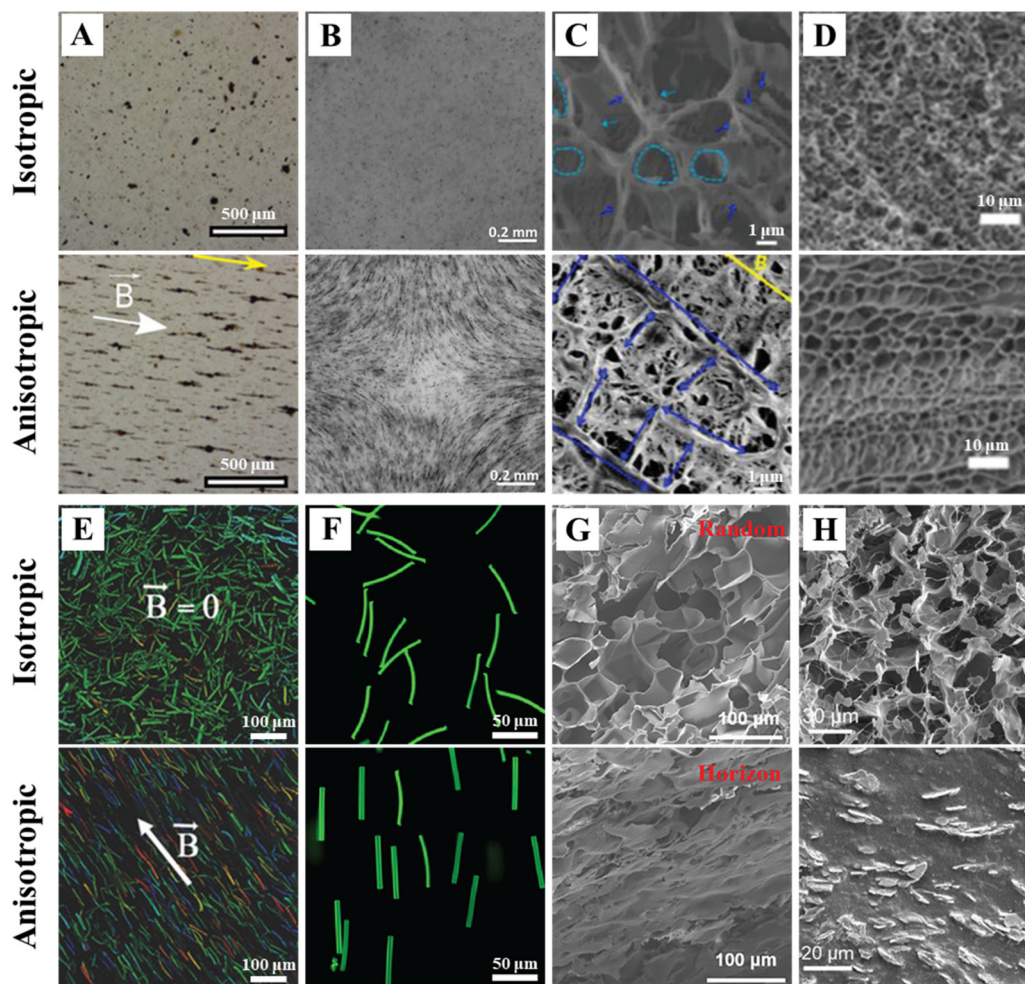
Fig. 2 Microscopy images of magnetically anisotropic hydrogels prepared by magneto-induced self-assembly. (A) Time-lapsed image of the growing filaments of MNPs in GelMA solution under static conditions and a 0.02 Tesla magnetostatic field for 30 min, respectively.[55] (Reprinted with permission from Wiley, copyright 2018.) (B) Bright-field images of GelMA hydrogels containing Fe_3O_4@SiO_2 nanorods under static conditions and a 7.5 mT electromagnetic field for 5 min, respectively.[59] (Reprinted with permission from Wiley, copyright 2023.) (C) Cryo-SEM images of polyisocyanide hydrogels containing iron oxide nanorods under static conditions and a 20 mT magnetostatic field for 2 min each in two perpendicular directions, respectively.[36] (Reprinted with permission from Wiley, copyright 2022.) (D) SEM images of freeze-dried gelatin containing MNP-decorated cellulose nanocrystals under static conditions and a 108 mT magnetostatic field for 90 min, respectively.[56] (Reprinted with permission from American Chemical Society, copyright 2019.) (E) Depth color-coded images of 3D fibrin hydrogels containing PLGA-based magnetic fibers under static conditions and a 100 mT magnetic field, respectively.[65] (Reprinted with permission from Wiley, copyright 2017.) (F) Optical microscopy images of rod-shaped poly(ethylene oxide-stat-propylene oxide) microgels containing superparamagnetic iron oxide nanoparticles under static conditions and a 100 mT magnetic field, respectively.[37] (Reprinted with permission from American Chemical Society, copyright 2017). (G) Representative SEM images of hydrogels containing PNIPAm-MoS_2/Fe_3O_4 nanosheets under static conditions and a 1 T electromagnetic field, respectively.[58] (Reprinted with permission from Wiley, copyright 2022.) (H) SEM images of hybrid hydrogels containing Fe/Al_2O_3 platelets under static conditions and a 300 mT magnetic field.[66] (Reprinted with permission from Elsevier 2022.)

dynamic range of the hydrogel, but also generates modulus gradients in a specific location. Chen *et al.*[36] developed hydrogels with graded anisotropic structures containing magnetic nanorods prepared by a simple one-step *in situ* method under low magnetic fields (Fig. 2C). It is worth noting that although most magnetic nanomaterials exhibit good biocompatibility, it is generally not biologically feasible to prepare magnetically anisotropic hydrogels by adding fully magnetic 1D materials, which may be because the concentration of MNPs in hydrogels exceeds their critical toxic concentrations.[60–62]

In order to avoid the cytotoxic effects of fully magnetic 1D materials, the strategy of combining biocompatible nonmagnetic anisotropic elements with MNPs to construct anisotropic structures has been proposed. For example, Araújo-Custódio *et al.*[56] prepared hybrid magnetic nanorods by co-precipitating iron oxide on rod-shaped cellulose nanocrystals. The obtained magnetic nanorods (0.1–0.5 wt%) were incorporated within the hydrogel matrix, and a uniform low magnetic field (108 mT) was used to induce a magnetic nanomaterial alignment (Fig. 1C and 2D). The resulting magneto-responsive hydrogels

with bioinspired directional microstructures showed a better biological performance and anisotropic mechanical properties. Sommer et al.[63] coated the surface of calcium sulfate rods with superparamagnetic iron oxide nanoparticles to endow them with magnetic responsiveness, and then induced controlled anisotropic porosity in hydrogels by using aligned magnetic rods as sacrificial templates. Moreover, MNPs can also be incorporated into the internal structure of 1D nonmagnetic anisotropic elements rather than being bound to the surface, which is more conducive to improving the colloidal stability. Liu et al.[64] fabricated magnetic microcryogels with pre-defined shapes by cryogelation and micro-molding technologies, which can be controllably assembled from bottom to top under a magnetic force to generate magnetically anisotropic hydrogels. Electrospinning is also an effective strategy for preparing magnetic fibers used as nanofillers to design ordered structures. Johnson et al.[57] reported that SPIONs were incorporated into poly-L-lactic acid solutions and magnetic electrospun fibers were prepared by electrospinning/microcutting techniques (Fig. 1D). The obtained fibers were added into collagen and aligned under the application of magnetic fields, which could provide directional guidance to the internal neurons.

2.3 Self-assembly of 2D magnetic nanomaterials

Hydrogels filled with 2D nanomaterials have attracted great interest due to their excellent mechanical properties and optimized functionalities.[67] Additionally, the incorporation of 2D nanomaterials into hydrogels can be used to develop novel functions through shear stress, mechanical stretching or electric field-induced assembly.[68,69] Drawing inspiration from these developments, the combination of MNPs with 2D nanomaterials has emerged as a promising strategy for the fabrication of high-performance magnetic anisotropic hydrogels. Here, the magneto-induced self-assembly of 2D nanomaterials with magnetic responsiveness in the hydrogel matrix is discussed.

Chen et al.[58] developed a programmable hydrogel with a controllable anisotropic structure. 2D nanomaterials with both magnetic and photothermal stimuli-responsiveness were fabricated through co-precipitating Fe_3O_4 and anchoring poly(N-isopropyl acrylamide) (PNIPAm) on the surface of MoS_2 nanosheets prepared by a liquid-phase exfoliation method (Fig. 1E and 2G). The resulting hydrogel cubes prepared by 3D printing were oriented in a horizontal magnetic field environment. Based on the magneto- and NIR photo-responsive properties of the nanosheets, local control of the thermal-induced phase transition within the 3D-printed hydrogels was achieved, leading to the development of a remarkable gel with a 2D barcode array direction. Apart from surface-coated magnetic materials, anti-magnetic nanomaterials can also be aligned in an ordered manner using a magnetic field. Due to the anti-magnetic "ring current" effect of the π-conjugated system, graphene oxide (GO) nanosheets are typical anti-magnetic materials that can be aligned parallel to the plane of a strong magnetic field to prepare magnetic anisotropic hydrogels.[70] Wu et al.[71] utilized the magnetic-induced orientation of GO

and in situ crosslinking polymerization of acrylic acid monomers to prepare a highly anisotropic hydrogel with rheological anisotropy. The formation of the gel network effectively suppressed the structural relaxation of GO, and the anisotropic structure was preserved even without a magnetic field, facilitating the in situ chemical reduction of GO. The anisotropic hydrogel hybridized with reduced graphene oxide (RGO) exhibited anisotropic enhanced conductivity.

3. The versatility of magnetically anisotropic hydrogels

Hydrogels with anisotropic structures often display unique mechanical, thermal, optical, electrical, and biological properties. These properties stem from the directional alignment of the constituent molecules or particles. Magnetic field, as an important physical field, provides a novel strategy with multiple advantages for achieving the directional alignment of magnetic nanomaterials. The magneto-induced self-assembly imparts anisotropic properties and novel performances to hydrogels. Such hydrogels have drawn significant attention for a wide range of applications, from tissue engineering to sensors and actuators.

3.1 The effect of magnetically anisotropic cues on hydrogels' mechanical properties

Despite the excellent biocompatibility of hydrogels, their weak mechanical strength can only match a few biological tissues, limiting their widespread application in the field of tissue engineering.[76] Research studies have shown that linearly arranged fillers can better mimic the morphology and mechanical properties of biological tissues.[77,78] Anisotropic hydrogels containing such fillers exhibit excellent compression strength in the orientation direction, attributed to the enhanced stress transfer between the nanofillers.[79,80] The magnetic alignment capability of magnetic nanofillers under magnetic stimulation has been widely used to prepare magnetically anisotropic hydrogels with mechanical properties mimicking human tissues.

Araujo Custódió et al.[56] prepared magnetic fibers by co-precipitating MNPs on rod-like cellulose, and achieved their alignment within a gelatin-based hydrogel under a 108 mT magnetic field. The ordered orientation of the magnetic fibers in the hydrogels maximized the storage modulus along their main axis, resulting in highly anisotropic mechanical properties of the hydrogels. Liu et al.[66] fabricated a novel multistimuli-responsive anisotropic hydrogel by copolymerizing superparamagnetic nanoparticle-coated alumina platelets (Fe/Al_2O_3), and N-isopropylacrylamide (NIPA) under a uniform magnetic field (Fig. 2H and 3A). The aligned magnetic platelets within the hydrogels endowed them with unique anisotropic mechanical properties. Specifically, the hydrogel exhibits a higher fracture stress and elongation ratio in the direction parallel to the magnetic field, which can be attributed to the oriented magnetic platelets acting as crack bridges to resist
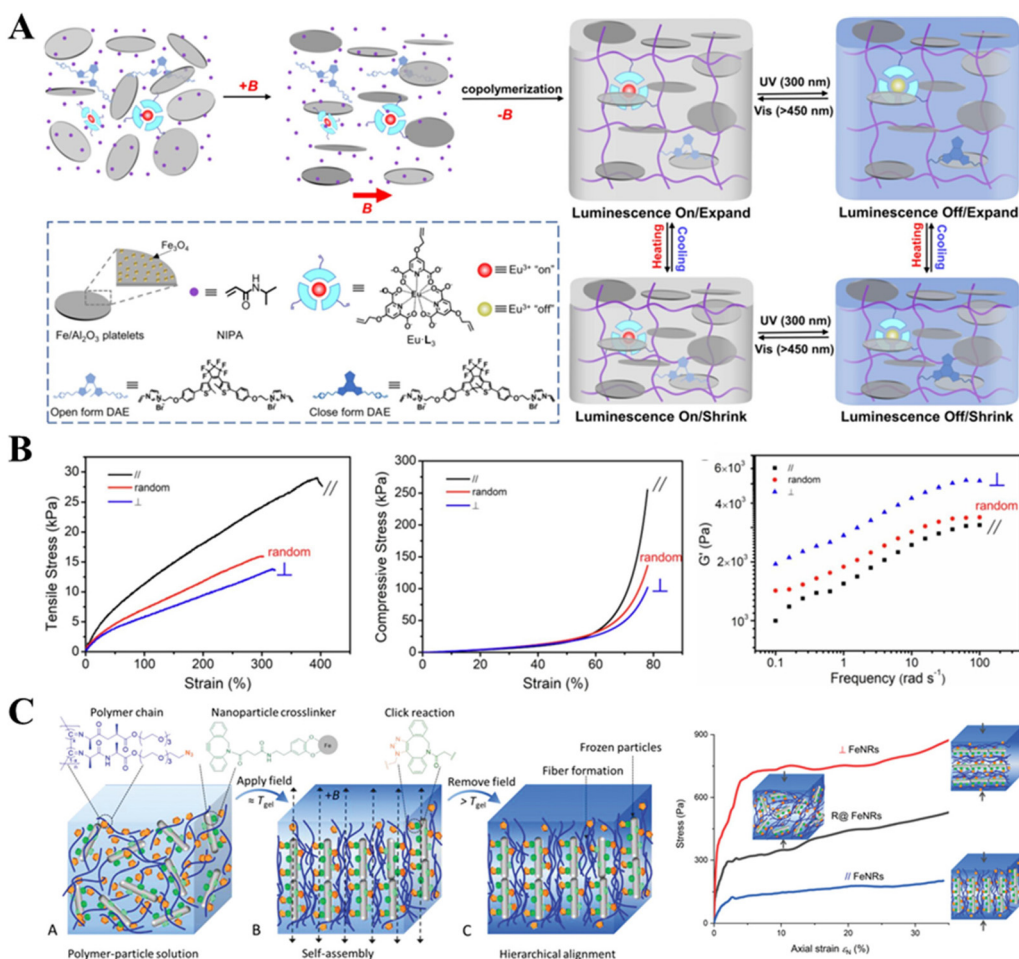
Fig. 3 (A) Schematic illustration for the construction of the hybrid hydrogel with multi-stimuli-responsive mechanical/luminescent dual anisotropic properties. (B) Tensile stress strain curves, compression stress strain curves and storage modulus of the hybrid hydrogel (from left to right).[66] (Reprinted with permission from Elsevier, copyright 2022.) (C) Schematic diagram of the preparation and assembly of magnetically anisotropic polyisocyanide, and mechanical anisotropy of composite hydrogels.[36] (Reprinted with permission from Wiley, copyright 2022.)

the propagation of cracks and dissipate mechanical energy during the deformation, thus preventing further damage. Moreover, the compressive strength and storage modulus parallel to the magnetic field direction were found to be 2.5 times and 2 times higher, respectively, than those measured in the direction perpendicular to the magnetic field (Fig. 3B). This difference can be attributed to the fact that compression perpendicular to the magnetic platelets mainly occurs in the soft polymer matrix, whereas compression parallel to the magnetic platelets requires overcoming the resistance caused by the folding and breaking of the nanosheets. However, Chen *et al.*[36] obtained opposite results, in which Young's modulus of a hydrogel perpendicular to the MNP alignment direction ($E_\perp$ = 952 Pa) was much higher than that parallel to the MNP alignment direction ($E_\parallel$ = 386 Pa) under large strain conditions (Fig. 3C). The underlying physical mechanism behind this difference is considered to be related to the morphologies of magnetic materials, the properties of the hydrogel matrix, the crosslinking strategy, *etc*. It prompts that many factors should

be simultaneously considered when designing magnetic anisotropic hydrogels.

3.2 The effect of magnetically anisotropic cues on hydrogels' thermal properties

Heat is an important physical factor in biology and medicine. The introduction of heat makes hydrogels more biocompatible, comfortable, and safe, which is evidently necessary for the tissue reconstruction process after damage. Additionally, if the hydrogel is loaded with drugs, it can also achieve thermally-controlled drug release.[81–83] The unique magnetothermal effect of magnetic materials endows them with innate advantages in biomedical domain.[84] The mechanism and regulatory strategies of the magnetothermal effect have been systematically studied. However, most of the magnetic hydrogels currently used for magnetothermal therapy did not consider the ordered arrangement of magnetic materials, which may suggest novel and unique properties and functionalities.
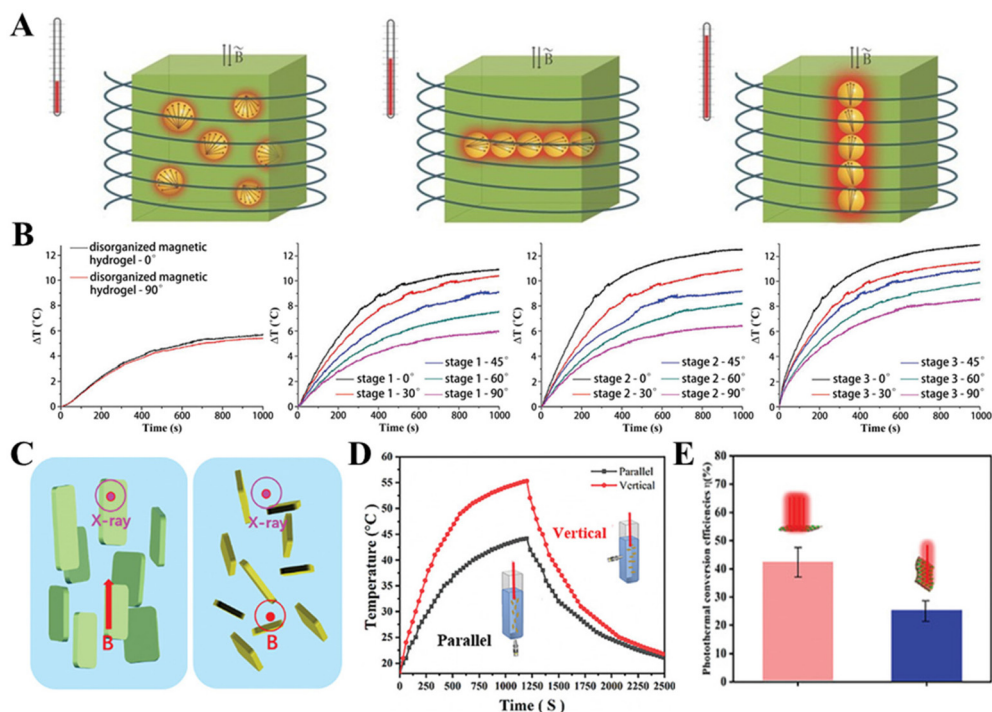
Fig. 4 (A) Schematic cartoon of the magnetothermal effect for the disorganized sample and the aligned magnetic sample in two directions. (B) Magnetothermal curves of the disorganized magnetic hydrogel and aligned magnetic hydrogel with chains immobilized at 3, 15, and 45 min, respectively (from left to right). The included angle between the chains and the applied alternating magnetic field was 0°, 30°, 45°, 60°, and 90°.[38] (Reprinted with permission from Wiley, copyright 2015.) (C) Schematic illustration of the photothermal test of arranged magnetic hydrogels under perpendicular and parallel X-ray irradiation. (D) Temperature profiles of MoS_2/Fe_3O_4 solution over time by placing a magnetic field parallel and vertical to NIR light illumination for the beginning 1200 s. (E) Photothermal conversion efficiency of PNIPAm-MoS_2/Fe_3O_4 hydrogels under the magnetic field of different directions.[58] (Reprinted with permission from Wiley, copyright 2022.)

Through magnetically assembling magnetic nanospheres within hydrogels, Hu et al.[38] achieved enhanced heat generation, and the resulting magnetically anisotropic hydrogels exhibited direction-dependent heating under an alternating magnetic field (Fig. 4A). The magnetic coupling between nanospheres restricts the reversal of homologous magnetic moments, hence the alternating magnetic field must consume more energy to drive the reversal of magnetic moments. The magnetic coupling along the chain direction is much stronger than that perpendicular to the chain direction. Therefore, the heat generated by an alternating magnetic field parallel to the direction of the chain is greater than that generated by a field perpendicular to the chain direction (Fig. 4B). A more general result shows that the magnetothermal efficiency is inversely proportional to the angle between the chain and the alternating magnetic field. Moreover, a recent study utilized thermo-responsive poly(N-isopropylacrylamide) (PNIPAm) and magnetic nanoplatelets (MoS_2/Fe_3O_4) to prepare a novel programmable anisotropic material with magnetic and photothermal responsive properties (Fig. 4C).[58] The photothermal effect of MoS_2 nanosheets results in a rapid increase in the temperature of the MoS_2/Fe_3O_4 gel under near-infrared light irradiation (Fig. 4D). And changing the orientation of magnetic nanoplatelets results in significant variations in their photothermal efficiency and optical properties. Specifically, the near-infrared

light irradiation perpendicular to the magnetic field exhibits higher photothermal efficiency compared with the parallel irradiation (Fig. 4E). These results indicate that the anisotropic hydrogels fabricated by magneto-induced self-assembly have adjustable thermal properties, and have great application potential in precise therapy and information storage.

3.3 The effect of magnetically anisotropic cues on hydrogels' optical/electrical properties

Traditional hydrogels usually lack conductivity, which limits their ability to mimic the physiological microenvironment of electrically active tissues such as skeletal, cardiac, and neural tissues.[85] The most common method for producing conductive hydrogels is to incorporate conductive nanoparticles into the polymer matrix. Compared to hydrogels carrying randomly distributed conductive nanoparticles, hydrogels containing oriented aligned nanoparticles exhibit significantly enhanced electrical conductivity.[86] Based on the advantages of the long-range regulation of magnetic fields, the preparation of conductive hydrogels with oriented structures by combining conductive and magnetic materials has become a current research hotspot. For instance, Liu et al.[39] utilized an external magnetic field to align anisotropically a magnetic fluid composed of polydopamine-coated carbon nanotube-Fe_3O_4 hybrids (PFeCNT), and then solidified this anisotropic structure via
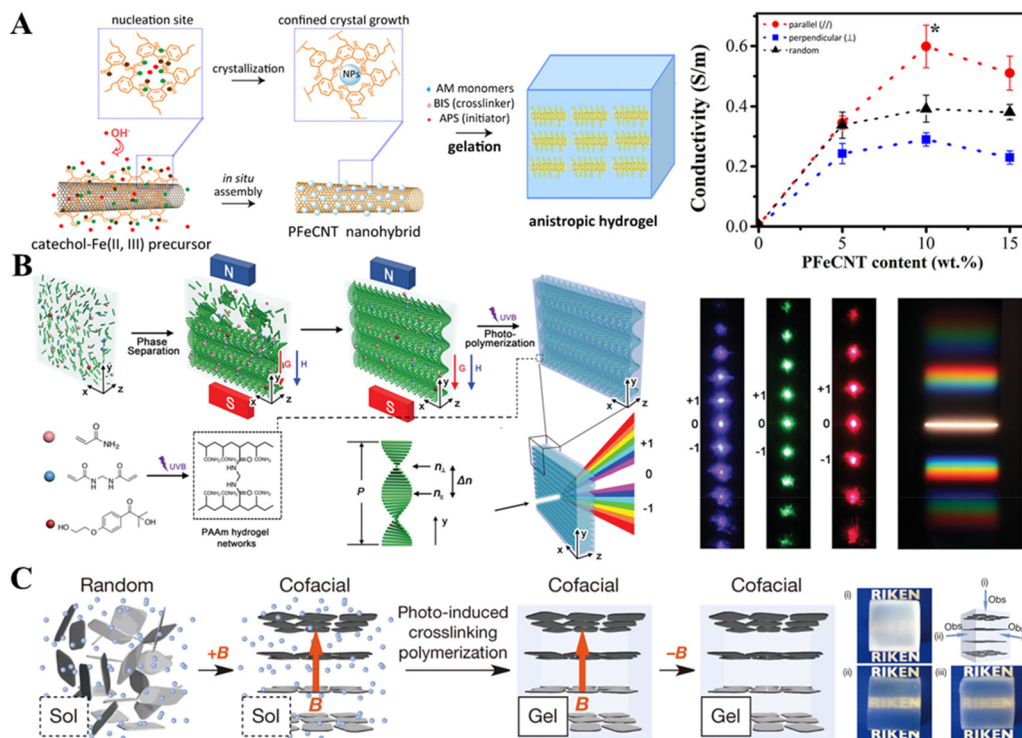
Fig. 5 (A) Schematics of the preparation of an anisotropic hydrogel based on a mussel-inspired conductive ferrofluid, and effects of the ordered PFeCNT nanohybrids on the anisotropic conductivity of the hydrogels.[39] (Reprinted with permission from American Chemical Society, copyright 2019.) (B) Schematic representation of the formation of the optical grating hydrogel. Images of the transmission diffraction pattern of incident monochromatic blue laser light (450 nm), green laser light (523 nm) and red laser light (650 nm), white light shone through a rectangular slit (from left to right).[74] (Reprinted with permission from Wiley, copyright 2020.) (C) Structural and optical anisotropic features of hydrogels containing cofacially oriented TiNSs in a quasi-crystalline order.[75] (Reprinted with permission from Springer Nature, copyright 2015.)

in situ free radical polymerization of acrylamide monomers for gelation (Fig. 5A). The anisotropic hydrogel based on conductive ferrofluid exhibits direction-specific conductivity. Compared to the vertical direction, the electrical conductivity parallel to the direction of PFeCNT was significantly enhanced due to the more complete path of electroosmotic flow. The enhancement in conductivity is attributed to the CNT network aligned parallel to the direction of the applied electric field, which facilitates the propagation of current. Ahadian *et al.*[87] prepared a gelatin-based hydrogel containing aligned CNTs using a dielectrophoresis approach, which exhibits conductivity more than 15 times greater than that with randomly oriented CNTs. The developed magnetic anisotropic hydrogels possess tunable mechanical and electrical properties, providing an effective and controllable platform for the electrical stimulation and differentiation of stem cells, with potential applications in tissue regeneration and cell therapy.

In addition, studies have shown that the magnetically induced 1D assembly of magnetic colloidal particles can produce photonic crystal structures, which can display structural colors in the visible light range. Significant progress has been made in constructing and fixing photonic structures using gelation properties and magnetically induced self-assembly.[88–90] For example, Wang *et al.*[91] utilized the magneto-induced self-assembly of carbon-encapsulated mag-

netic nanoparticles to prepare a photonic chain structure, resulting in the preparation of a structurally colored hydrogel with sensitivity to temperature and ionic strength. Cao *et al.*[74] reported a simple method for fabricating gratings by using the synergistic effects of gravity-induced phase separation and magnetic field-induced orientation of cellulose nanocrystals (CNCs), which were fixed in a polymer network *via* photopolymerization to obtain hydrogel films with uniform periodic structures arranged perpendicularly (Fig. 5B). The developed hydrogel generates up to sixth-order diffraction spots and shows linear polarization selectivity. Under a strong magnetic field, Liu *et al.*[75] achieved the co-alignment of negatively charged unilamellar titanate and fixed this transversely induced ordered structure *in situ via* photo-triggered vinyl polymerization (Fig. 5C). The optical transparency of hydrogels with anisotropic structures is significantly higher in the direction orthogonal to the magnetic flux than in the parallel direction. Materials with optical anisotropy induced by magnetic orientation have great potential in many fields, such as organic light emitting diodes and field emission devices.

3.4 The effect of magnetically anisotropic cues on cell behavior

Magnetism has become a frequently used tool for preparing anisotropic hydrogels with complex structures that mimic

natural human tissues. In addition to inducing the oriented arrangement of magnetic materials, magnetic fields themselves also exert significant effects on biological systems.[40,52] In particular, when combined with an external magnetic field, the subtle deformation of magnetic materials can directly transmit mechanical stimuli to cells, activating mechanosensitive receptors and thereby affecting cell activity and controlling their behavior.[92–95] Overall, the application of an external magnetic field can be used both to create anisotropic hydrogels and to remotely stimulate encapsulated cells. Furthermore, the combination of magnetic anisotropic hydrogels and magnetic stimulation allows for a higher degree of mimicking the anisotropic physical/mechanical properties of natural tissues, while also enabling remote mechanical stimulation of encapsulated/implanted cells at the relevant cellular scale.[96,97] The comprehensive control of the structure of biological materials and driving of biological components by magnetism represents a key advantage of this approach.

Araújo-Custódio et al.[56] prepared magnetic anisotropic hydrogels using magnetic nanorods and observed directional growth of both seeded cells on the hydrogel surface and encapsulated cells within the hydrogel (Fig. 6A). The authors speculate that the rigid nanoparticles in the soft gelatin matrix provide nanotopographical cues for cell–substrate adhesion and actin extension and contraction, thereby promoting cell spreading in a particular direction. However, when 0.3 wt% nanoparticles are used, the directional growth behavior disappears, which suggests that there is a best material design to achieve cell alignment (Fig. 6B). In addition, it has been demonstrated that incorporating PEG-terminated magnetic nanoparticles in a directional arrangement can improve cell viability during UV crosslinking of hydrogels (Fig. 6C).[55] Echave et al.[98] reported an enzymatically crosslinked gelatin hydrogel with anisotropic features, where a tunable magnetostatic field was used to trigger the alignment of CNC in a hydrogel network. The cells embedded in the anisotropic system grew directionally along the aligned CNC, and the sharp peaks at specific angles were noticed, obtaining values of the full with half medium (FWHM) around 60° (Fig. 6D). Notably, the strength of the magnetic field used to fabricate anisotropic structures had no significant effect on cell organization (Fig. 6E). Moreover, Goodrich et al.[59] created a non-uniform stiffness field in a single hydrogel containing MNRs using an anisotropic magnetic field, and investigated the local modulus dependence of iPSC differentiation. The results showed that cells in hydrogels with pre-aligned magnetic rods exhibited the greatest expression of active-RhoA and YAP, both of which are mechanical stimulation-sensitive proteins,
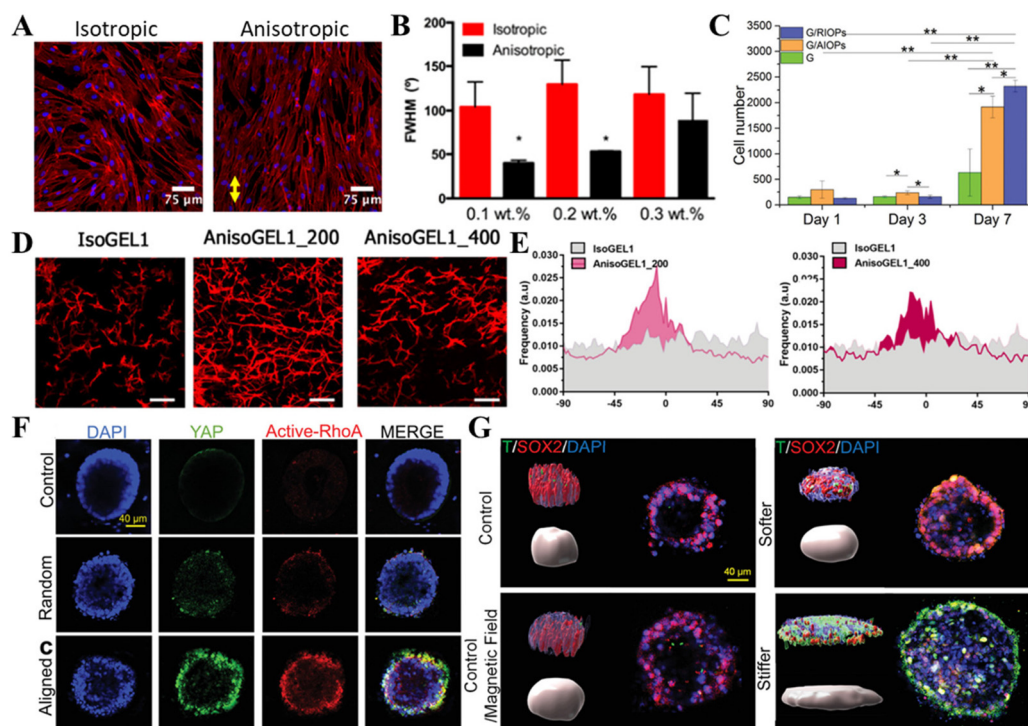
Fig. 6 (A) Representative images of hASCs seeded on isotropic and anisotropic hydrogels after 3 days of culture (red, cytoskeleton; blue, nucleus). (B) The full with half medium (FWHM) of the distribution was calculated for cells seeded on hydrogels.[56] (Reprinted with permission from American Chemical Society, copyright 2019.) (C) The viability of the cells encapsulated in 3D hydrogels at day 1, 3, and 7.[55] (Reprinted with permission from Wiley, copyright 2018.) (D) Confocal fluorescence images of the cellular cytoskeleton (F-actin, red) encapsulated in 3D hydrogels. Scale bars = 200 μm. (E) The directionality histograms of actin filament distribution after 1 week of culture.[98] (Reprinted with permission from American Chemical Society, copyright 2019.) (F) The effects of hydrogel stiffening on the mechano-sensitive RhoA signaling of iPSCs cultured within a MNR-incorporated hydrogel. (G) The effects of the local modulus on the differentiation of iPSCs.[59] (Reprinted with permission from Wiley, copyright 2023.)

suggesting a superior dynamic range of the hydrogel with pre-aligned MNRs (Fig. 6F). Moreover, in the stiffer region, the cells formed a discoidal colony with a higher expression of the mesodermal marker brachyury and a mild expression of SOX2, an ectodermal marker (Fig. 6G). This magnetic-responsive hydrogel system can serve as a platform for investigating the biological behaviors of cells in dynamic mechanical microenvironments.

To conclude, the anisotropic structural properties of scaffolds serve as crucial biophysical cues that activate intracellular biochemical signals, which in turn regulate various functional processes of encapsulated or inoculated cells, including growth, migration, and in the case of stem cells, differentiation into specific lineages.

4. Tissue engineering applications of magnetically anisotropic hydrogels

Many biological tissues in the human body exhibit complex anisotropic structures from micro to macro scales, which make them difficult to repair after damage. The ultimate aim of regenerative strategies is to activate the natural repair process in tissue engineering systems, guiding the formation of new tissues and restoring their original function. Apart from geometric cues, mechanical stimuli play a crucial role in the epigenetic control of tissue development, remodeling, and regeneration, which has been demonstrated to significantly enhance the *in vitro* maturation performance of tissue-engineered constructs. Magnetically anisotropic hydrogels not only provide well-organized 3D templates that can replicate the complex structural properties of natural tissues, but also can deliver magneto-mechanical stimuli to cells to regulate their biological behavior under external magnetic fields. Given these aspects, magnetically anisotropic hydrogels can provide the desired anisotropic properties for the fabricated tissue engineering scaffolds and offer on-demand remote mechanical stimuli in tissue engineering strategies. In this section, we review the application of magnetically anisotropic hydrogels in tissue engineering strategies to simulate different specific tissues, including skeletal muscle, cartilage, tendon, and neural tissue.

4.1 Application in skeletal muscle tissue engineering

Skeletal muscle is a complex structure composed of muscle fiber bundles. It is the largest and strongest muscle system in the human body, playing a crucial role in improving physical performance and fitness level.[99] Each muscle fiber bundle consists of many multinucleated muscle fibers, characterized by their elongated morphology and tubular structure (Fig. 7A). As the basic unit of muscle contraction, myofibers are composed of proteins such as myosin and creatine kinase, and have a high degree of uniaxial arrangement along the main axis of the tissue.[100,101] Different types of muscle fibers exhibit structural and functional differences, such as fast-twitch fibers being suitable for explosive strength and slow-twitch fibers being suitable for sustained low-intensity exercise. The anisotropic structure of skeletal muscle results in different mechanical and electrical properties in different directions, enabling our bodies to perform different movements.[21,102]

The strategy of muscle tissue engineering focuses on designing structurally anisotropic scaffolds that provide sufficient features for cell growth, alignment, and functional differentiation. Recently, oriented micro/nanofibers as fillers combined with natural or synthetic polymers have been proposed to construct muscle tissue engineering scaffolds with anisotropic properties, and have been widely studied. Magnetically anisotropic hydrogels have also been investigated as potential scaffold materials to achieve the desired contractile function of skeletal muscle tissues. For instance, an anisotropic hydrogel containing aligned electromagnetic nanohybrids has been developed to guide the directional migration and growth of C2C12 cells.[39] And the myoblasts exhibited the most pronounced oriented growth under electrical stimuli, because the current signal stimulates the cells most significantly along the direction of the conductive ferrofluid. Furthermore, the ordered hydrogels combined with electrical stimuli enhanced the directional accumulation of vinculin, which plays an important role in maintaining the myofiber morphology, muscle tension transmission, and muscle cell structure. The results demonstrated that magneto-induced anisotropic conductive hydrogels have great application potential in skeletal muscle tissue engineering. In another work, the authors prepared cellularized anisotropic scaffolds by a magneto-induced arrangement of MNPs in gelatin-based hydrogels.[55] The results showed that C2C12 cells grew directionally along the aligned magnetic filaments within anisotropic hydrogels within 72 hours (Fig. 7B). Compared to the other groups, C2C12 cells in the magnetically anisotropic hydrogel showed higher myosin heavy chain (MyHC) expression and enhanced myotube formation in the elongated structures, which was further promoted by adding a differentiation medium (Fig. 7C). The characteristic of magnetically anisotropic hydrogels, *i.e.*, inducing the differentiation of C2C12 cells in mature multinucleated myotubes, provides ideas for the fabrication of novel scaffolds for skeletal muscle tissue engineering. In addition, Wang *et al.* prepared novel magnetic controlled short nanofibers (MSNFs) using an advanced coaxial electrospinning–cyrocutting approach, and further designed an injectable aligned MSNF/gel scaffold *via* a remote magnetic field.[73] The developed anisotropic MSNF/gel scaffolds significantly promoted the formation of newborn myofibers and accelerated angiogenesis and tissue remodeling in a rat volumetric muscle loss (VML) model (Fig. 7D). Moreover, compared with the blank group, the anisotropic MSNF/gel scaffold group exhibited more parallel and longer myofibers with a well-organized structure, indicating that the magnetic alignment provided an anisotropic microenvironment for skeletal muscle regeneration (Fig. 7E). This approach offers a new promising tissue engineering strategy for the aligned myofiber formation for enhancing skeletal muscle regeneration *in vivo*.
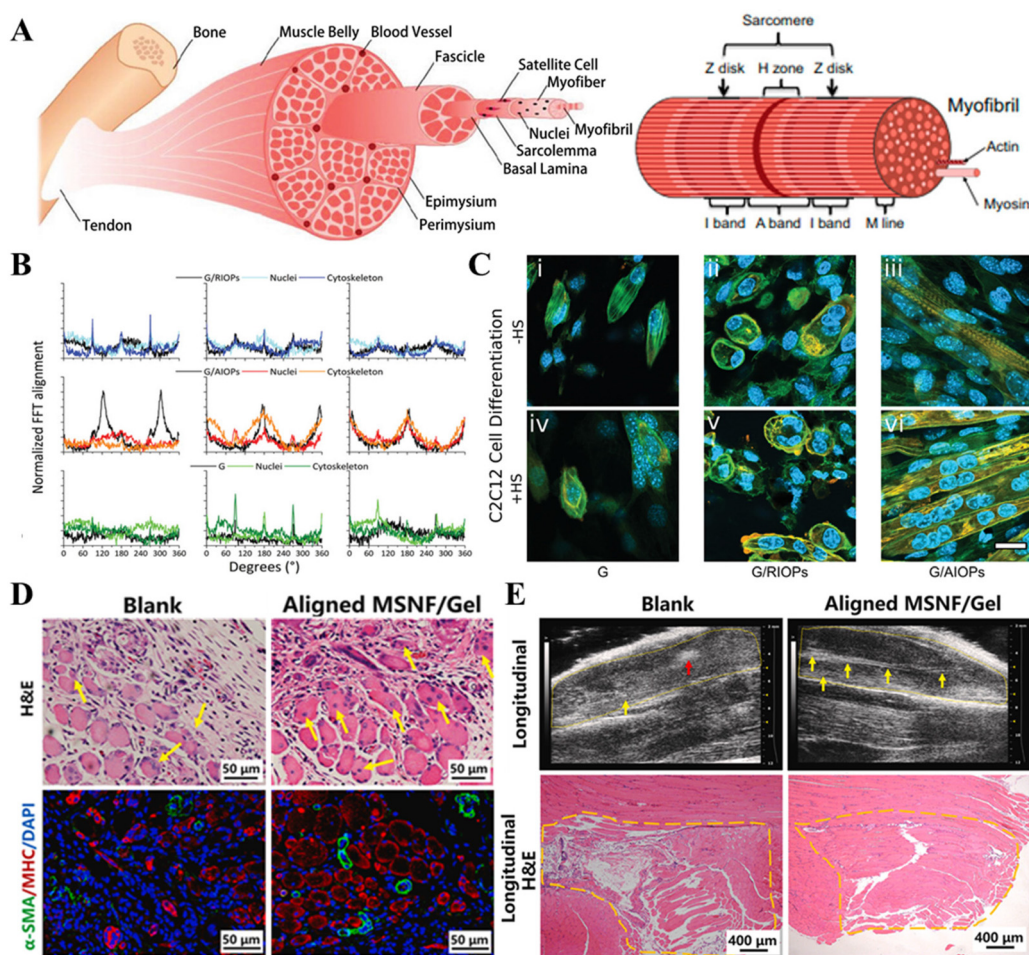
Fig. 7 (A) The hierarchical structure of skeletal muscle, wherein fibers are bundled together in increasingly larger fascicles.[21,99] (Reprinted with permission from American Chemical Society and Wiley, copyright 2021 and 2020, respectively.) (B) 2D-FFT analysis of the fluorescent images at day 1, 3, and 7. (C) Immunofluorescence images of C2C12 cells embedded in different hydrogels cultured in the presence and absence of horse serum (HS) at day 11. Nuclei (DAPI, blue), actin filaments (Phalloidin, green), and myosin filaments (myosin heavy chain (MyHC), orange). Scale bars = 20 μm.[55] (Reprinted with permission from Wiley, copyright 2018.) (D) Skeletal muscle regeneration in a rat VML model after implantation of aligned a MSNF/gel scaffold for 1 week. Yellow arrows in the image showing H&E staining indicate centronucleated myofibers, immunofluorescence staining of the tissue sections of α-smooth muscle actin (α-SMA, green) and the myosin heavy chain (MHC, red) to assess angiogenesis and tissue remodeling. (E) Ultrasound images and H&E staining of the defective area of rats treated with an aligned magnetic scaffold after 2 weeks and 8 weeks, respectively. The yellow boxes indicate the defective area, the red arrow indicates the fibrous scar tissues and the yellow arrows indicated the regenerated myofibers.[73] (Reprinted with permission from Elsevier, copyright 2022.)

4.2 Application in cartilage tissue engineering

Cartilage is a special connective tissue rich in collagen and elastic fibers, providing a smooth and hard surface for joint movement and load transmission.[6] Chondrocytes are the only cell type in cartilage, primarily responsible for secreting and maintaining the cartilage matrix.[103] In the superficial layer of cartilage, collagen fibers are closely arranged parallel to the cartilage surface.[104] The middle layer of cartilage is composed of randomly oriented fibers, and the fibers are aligned perpendicular to the cartilage surface in the deepest area (Fig. 8A). The different orientations of collagen fibers in different layers provide the cartilage with an anisotropic structure and properties. Additionally, cartilage exhibits excellent compressive properties, with a higher compressive modulus compared to

other tissues. This is due to the hydration and arrangement of proteoglycan molecules, which allow cartilage to slowly bend and absorb energy under compressive loads, thereby protecting the joints and maintaining their normal function.[11,105]

Based on the natural heterogeneous structure of the cartilage tissue, researchers have constructed a variety of anisotropic hydrogels for the repair of cartilage damage. Yu *et al.* developed decellularized extracellular matrix-based anisotropic hydrogels by controlled diffusion.[106] The anisotropic hydrogel, as a biological scaffold, significantly promoted the chondrogenic differentiation of mesenchymal stem cells *in vitro* and efficiently accelerated the regeneration of damaged cartilage *in vivo*. In addition, mechanical stimulation has been considered as a powerful and effective strategy to enhance the unique properties of tissue engineered constructs because of
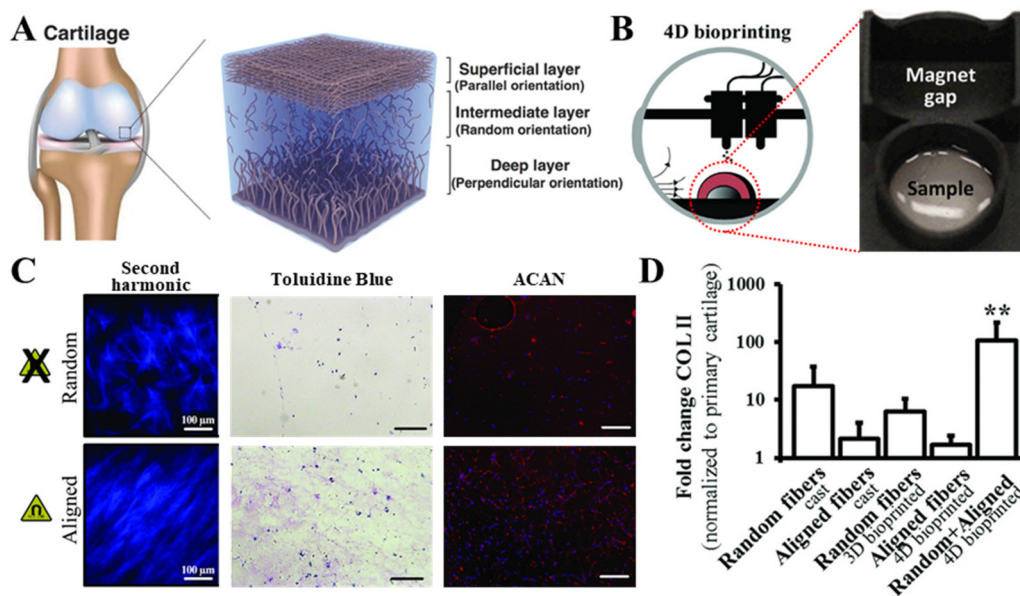
Fig. 8 (A) Schematic illustration of the highly ordered structures of cartilage.[6] (Reprinted with permission from Wiley, copyright 2017.) (B) 4D bioprinting stage including a custom-designed adaptor for incorporating a cylindrical magnet that forces real-time remodeling of the bioink while bioprinting. (C) Second-harmonic generation images showing the collagen fiber alignment in printable bioinks in the presence or absence of a magnetic field. Toluidine blue histological staining (scale bars = 100 μm) and aggrecan (ACAN) antibody staining (scale bars = 200 μm) of the bioprinted samples. (D) The expression analysis of COL II.[72] (Reprinted with permission from John Wiley and Sons Ltd, copyright 2018.)

the stress-growth properties of cartilage. Magneto-mechanical stimulation, as a new type of mechanical force, has attracted widespread attention and research due to its advantages such as fast response, deep tissue penetration, remote driving, and precise spatiotemporal regulation.[92] For example, Fuhrer et al.[107] prepared magnetic hydrogels by combining MNPs with styrene–maleic anhydride copolymers, and induced cyclic deformation of the soft magnetic hydrogel scaffold using an ultra-low frequency pulse magnetic field of 800 mT. The results demonstrated that the magneto-mechanical stimulation could induce chondrogenic differentiation of mesenchymal stem cells without any additional chondrogenic transcription factors. Moreover, magnetic materials possess unique advantages in constructing anisotropic structures, which have strong appeal for highly biomimetic approaches in cartilage tissue engineering. Simińska-Stanny et al.[108] utilized magnetic-assisted 3D printing technology to produce anisotropic bilayer composites using a collagen–gelatin hydrogel containing iron oxide nanoparticles under an extremely weak magnetic field (2 mT) (Fig. 8B). The collagen fibers were forced to orientate under the magnetic field, resulting in an ordered and aligned collagen fiber tissue. This anisotropic structure led to the hydrogel scaffold exhibiting anisotropic enhanced mechanical properties, with a significantly higher compression modulus in the fiber alignment direction (Fig. 8C). Compared to the randomly oriented scaffold, chondrocytes loaded on the magnetic anisotropic scaffold expressed more type II collagen, indicating the potential of the proposed concept for application in cartilage tissue engineering (Fig. 8D).

4.3 Application in tendon tissue engineering

Tendon is a kind of connective tissue composed mainly of dense type I collagen fibers arranged along the long axis of the tissue, connecting muscles to bones (Fig. 9A).[109] Additionally, the composition of tendons also contains type III, V, and XII collagen fibers, elastic fibers, and other extracellular matrix molecules. The hierarchical organization of above molecules endow tendons with anisotropic mechanical and viscoelastic properties, with the maximum load-bearing capacity along the direction of collagen fibers.[110,111] The main function of tendons is to transmit the contraction force of muscles to the bones, thereby allowing the body to move and maintain postural stability. Moreover, tendons help regulate the strength and stability of muscles and joints, as well as assist the body in absorbing impact and reverse forces.[2]

Since tendons are mechanically sensitive tissues, developing smart hydrogels with anisotropic structures that can respond to external magnetic stimuli with mechanical deformation is crucial for achieving functional tendon tissue engineering. Pesqueira et al.[112] prepared a tropoelastin-based magnetic spongy-like hydrogel with a quasi-anisotropic lamellar-like structure by an in situ precipitation approach. With the application of an oscillating magnetic field, the magnetic hydrogels effectively promoted the adhesion, spreading and migration of human tendon-derived cells, suggesting their potential in accelerating tendon tissue regeneration. Echave et al.[98] developed a multiphase hydrogel system, in which oriented cellulose nanocrystals (CNCs) were incorporated to mimic the tendon tissue (Fig. 9B). The hASCs encapsulated in
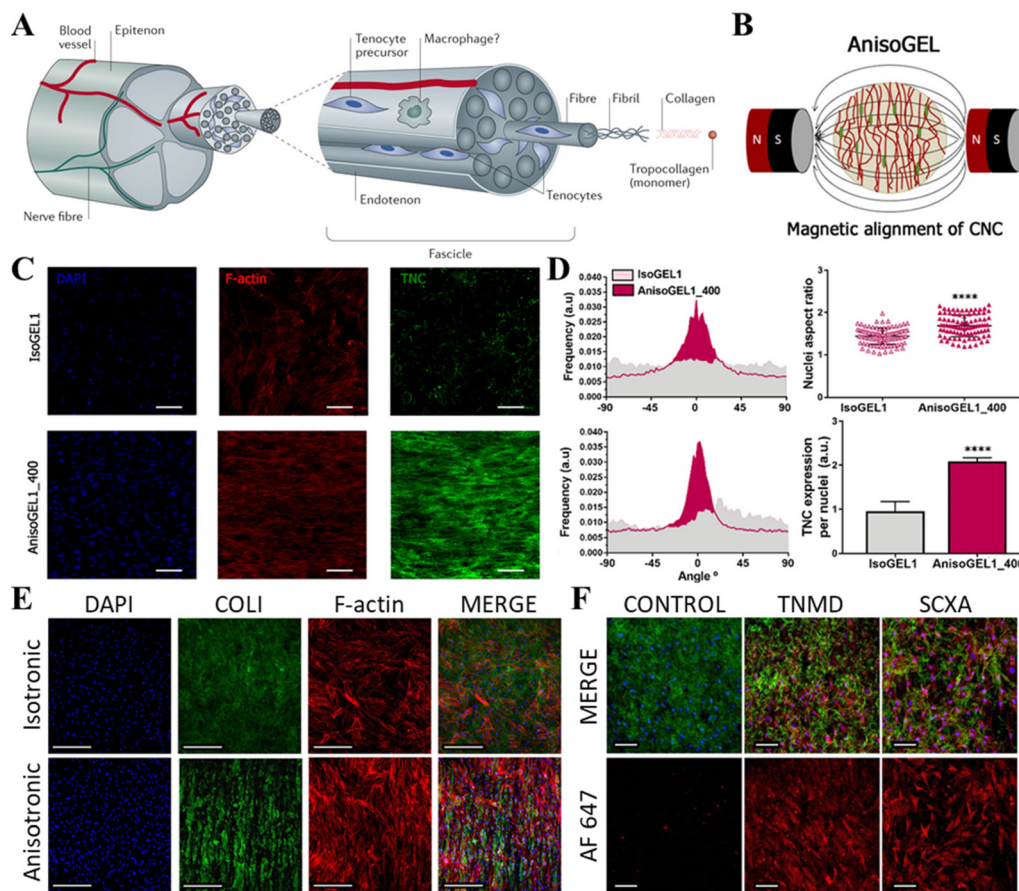
Fig. 9 (A) A cross-sectional view of a tendon showing the hierarchical structure of the organ at the tissue and molecular levels.[109] (Reprinted with permission from Springer Nature, copyright 2020.) (B) Schematic diagram of the magnetic alignment of CNC. (C) Confocal images of the immunolabeled samples against TNC (green), cell nuclei (blue), and cytoskeleton (red) (scale bars = 200 μm). (D) Evaluation of the TNC deposition (left top) and the cytoskeleton (left bottom) directionality by using the encapsulated cells; the nuclei aspect ratio of cells cultured in isotropic and anisotropic hydrogels (right top); and quantification of the tendon-related marker TNC expression normalized with the area of the nuclei (right bottom).[98] (Reprinted with permission from American Chemical Society, copyright 2019.) (E) Confocal imaging of primary hASCs seeded within collagen hydrogels 7 days post-seeding. Scale bars = 200 μm, blue = nuclei, red = F-actin, green = collagen I. (F) Confocal images of cellular collagen I scaffolds 7 days post-gelation following fixation and immunofluorescence staining for TNMD and SCXA. Scale bars = 100 μm, blue = nuclei, green = collagen I, red = TNMD or SCXA.[113] (Reprinted with permission from Frontiers Media S.A., copyright 2022).

magnetically anisotropic hydrogels exhibited an aligned cell growth, with a higher nuclear aspect ratio. In the anisotropic hydrogel, the expression of tendon-related ECM protein tenascin (TNC) was higher, and the deposition of this glycoprotein was shown in a more organized manner along the arranged CNCs (Fig. 9C and D). These results highlight the feasibility of using magnetically anisotropic hydrogels for developing tendon-mimicking connective tissues. Furthermore, Wright *et al.*[113] prepared collagen I hydrogels with anisotropic structures by adding anti-collagen I-labeled MNPs to a fluorescent collagen solution and immersing them in a 50–52 mT magnetostatic field for 30 min. It was observed that the F-actin filaments of hASCs seeded within the magnetically anisotropic hydrogel were unidirectional, parallel to the orientation of MNPs and fibrous collagen (Fig. 9E). And compared to the control group, the experimental group showed an increased expression of tenocyte-related proteins (tenomodulin (TNMD)

and scleraxis (SCXA)), confirming the tenocyte-likeness of the cells (Fig. 9F). These results demonstrated that the developed approach can be used to remotely control the collagen matrix organization, reproducing the natural tendons.

4.4 Application in nerve tissue engineering

Nervous tissue composed of neurons and neuroglial cells plays an important role in receiving, processing, and transmitting nerve impulses throughout the body.[114,115] Inside neurons, highly branched dendrites are connected through cell bodies to axons; an axon is a single long neural fiber that conducts signals one-way to other neurons or target cells (Fig. 10A). The axons are aligned in parallel bundles forming oriented axon tracts, which exhibit mechanical properties when arranged parallel or perpendicular to the shear displacement.[116] The anisotropic structure of neurons allows them to transmit nerve
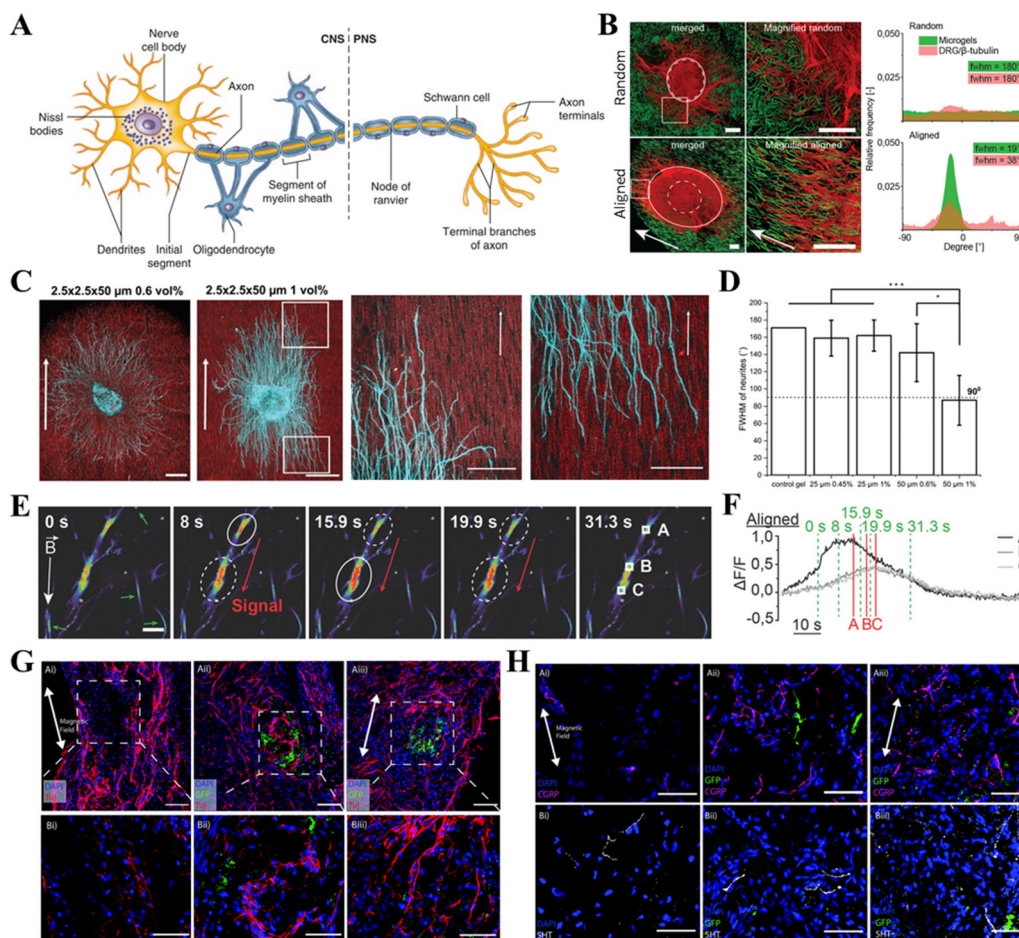
Fig. 10 (A) Schematic illustration of the structures of neurons.[114] (Reprinted with permission from Springer, copyright 2017.) (B) Fluorescent images of dorsal root ganglions (DRGs) positioned in hydrogels with microgels (green, fluorescein). Distribution of neurite and microgel orientation. Scale bars = 200 μm, β-tubulin staining (red, Alexa Fluor 633).[37] (Reprinted with permission from American Chemical Society, copyright 2017.) (C) Confocal micrographs of DRGs after seven days of culture in different anisogels (scale bars = 500 μm). Cyan indicates β-tubulin and red indicates rhodamine-labeled microgels, and the white arrows indicate the direction of alignment of the microgels. (D) Plot comparing the FWHM of neurite orientation under different microgel conditions.[119] (Reprinted with permission from Wiley, copyright 2022.) (E) The signal propagation direction of neurons cultured within the aligned magnetic hydrogel (scale bars = 20 μm). Red arrows indicate the calcium signal direction, while the small green arrows represent the fibers. The solid circle indicates a maintained or increasing signal, while the dashed circle corresponds to a fading signal. (F) Normalized quantification of the calcium signals in the aligned magnetic hydrogel.[65] (Reprinted with permission from Wiley, copyright 2017.) (G) Fluorescence images of axon infiltration in different scaffolds. Short scale = 100 μm, long scale = 50 μm. (H) Regeneration of sensory and serotonergic axons at the injury site. Scale = 50 μm; (i) aligned acellular, (ii) unaligned hMSC-seeded and (iii) aligned hMSC-seeded scaffolds. White arrows represent the direction of the magnetic field during surgery. DAPI (blue), GFP (green fluorescent protein, green), Tuj (red in (G)), CGRP (magenta in (H)), 5HT (serotonergic axon, white).[120] (Reprinted with permission from Royal Society of Chemistry, copyright 2022.)

impulses in different directions and improve the transmission efficiency of electrical signals, thereby realizing the complex functions of the brain and nervous system.[117,118]

Numerous studies have explored the use of self-assembly of magnetic materials in a magnetic field to manufacture hydrogels with anisotropic structures, providing guidance for directional growth of neurons and/or neural differentiation. For example, Rose *et al.*[37] reported a novel injectable PEG-based hydrogel involving rod-like magnetoceptive microgel objects that could be oriented at an external magnetic field of 130 mT. As a result, the cells responded strongly to the directional structure, leading to parallel nerve extension (Fig. 2F and 10B).

An anisotropic hydrogel was fabricated by combining MNPS and a weak magnetic field (25.5 mT), and its physical cues could induce the oriented growth of the encapsulated primary neurons and the development of co-oriented neurites of PC12, mimicking the cellular characteristics of the natural nerve tissue.[54] Moreover, collagen-based anisotropic hydrogels prepared based on the magnetic-responsive nanofibers have also been shown to provide directional nanotopographic cues for the arrangement of primary dorsal root ganglions, where the average length of cells is increased by 3 times.[57] Babu *et al.*[119] endowed hydrogels with anisotropic structures by using a weak magnetic field to induce a directional arrangement of mag-

netic microgels in PEG-based hydrogels. The *in vitro* experiments showed that 1 vol% microgels could significantly promote the directed growth of dorsal root neurons in chicken embryos, with a mean full width half medium (FWHM) of 87 ± 29°, representing a high level of neurite alignment (Fig. 10C and D). Omidinia-Anarkoli *et al.*[65] reported an injectable hydrogel with oriented magnetic fibers that can trigger axons to grow and extend unidirectionally along the fiber direction (Fig. 2E). Compared with pure hydrogels, hydrogels containing arranged or random staple fibers increased axon elongation by 55% and 34%, respectively, which facilitates the calcium signals propagating along the principal axis of the fibers (Fig. 10E and F). Furthermore, Tran *et al.* fabricated an anisotropic hydrogel utilizing a magnetically responsive self-assembling strategy, and verified its efficiency in promoting spinal cord injury repair *in vivo*.[120] Fig. 10G shows that the aligned hMSC-seeded scaffold significantly promoted the axon alignment along the rostral–caudal direction, which also efficiently augmented the regeneration of calcitonin gene-related peptides (CGRPs) (Fig. 10H). These results indicated that the developed magnetically aligned peptide hydrogel could provide topological cues to guide neurite growth and further accelerate the repair of the damaged spinal cord. With the advantages of inducing oriented growth of neurites and triggering unidirectional signal propagation along oriented nerves, magnetically anisotropic hydrogels show great application potential in nerve tissue engineering.

5. Conclusion and perspective

Biological tissues possess highly anisotropic mechanical and biological properties due to their unique structures, which are critical considerations in tissue engineering. Anisotropic hydrogels have become a perfect template material for constructing tissue engineering scaffolds due to their excellent biocompatibility and highly moldable properties. Magnetic self-assembly of materials can not only be used to construct magnetically anisotropic hydrogels, but also endow hydrogels with intelligent responsiveness to external magnetic fields, thereby regulating cellular behaviors. This provides a new design strategy for personalized clinical treatment based on tissue engineering. Currently, various magnetic nanomaterials with different magnetic properties (superparamagnetic, paramagnetic, diamagnetic, *etc.*) and structures (nanospheres, nanorods, nanowires, nanoplates, *etc.*) have been attempted for constructing magnetic anisotropic hydrogel materials. These successful attempts have endowed hydrogels with anisotropic mechanical, thermal, optical, and electrical properties and enabled the regulation of various types of cellular behaviors (neuronal cells, stem cells, fibroblasts, *etc.*) through the ordered anisotropic structure and magnetic responsiveness of magnetic anisotropic hydrogels. The potential applications of magnetic anisotropic hydrogels have been preliminarily demonstrated in various tissue engineering fields, such as cartilage, tendon, nerve, and skeletal muscle.

However, the application of magnetic anisotropic hydrogels in the biomedical field still faces many challenges. Firstly, although the tunable range of mechanical strength of magnetic anisotropic hydrogels has been greatly expanded (from Pa to MPa), it still cannot match all body tissues, such as bone tissue (GPa), the hardest tissue in the human body. Using magnetic-induced self-assembly to prepare novel ultra-high strength magnetic anisotropic hydrogels for bone tissue repair/strengthening will expand their application in bone tissue engineering. Secondly, the mechanism by which structural anisotropy in a 3D environment affects cellular behavior is not yet clear. Extensive research is still needed to identify the potential signaling pathways that govern the oriented morphology and migration of cells when cultured in anisotropic hydrogels. This is also a necessary step for the translation of cutting-edge research into clinical applications. Thirdly, biological tissues typically have a hierarchical structure with significantly different mechanical properties and biological activities between different layers, which cannot be simply mimicked by magnetic anisotropic hydrogels. To construct a fully biomimetic tissue engineering scaffold using magnetic anisotropic hydrogels, technological breakthroughs are needed. 3D bioprinting technology can finely control the three-dimensional structure of the construct, but only a few works have adopted this technique in the construction of magnetic anisotropic hydrogels. Additionally, many biological factors within the tissue have a decisive impact on cellular behavior, and the intrinsic mechanisms by which multiple factors (biological factors, anisotropic structure, external stimuli) synergistically affect cellular behavior need to be further clarified. Fourthly, the importance of the spatial characteristics of oriented domains, such as their size and distribution, in magnetic anisotropic hydrogels for achieving specific biological responses has not been fully elucidated. This may also become a bottleneck that limits the further clinical application of magnetic anisotropic hydrogels, and therefore further systematic research is needed. Fifthly, the magneto-mechanical stimulation is a novel means for remote real-time control of cellular behavior. By constructing magnetic anisotropic hydrogels, this concept can be further developed by considering additional effects such as light, electricity, and heat that arise from the ordered structure. The coupling between multiple effects may evolve into many important and interesting biological functions. Sixthly, although the influence of magnetic nanoparticles' size, shape, and other characteristics on cell fate has been widely studied, the conclusions are not always consistent. The relationship between the structure of magnetic nanoparticles and their biocompatibility has not been fully established. Meanwhile, the magnetic field intensity used in the construction of magnetic anisotropic hydrogels also needs to be carefully selected, as strong magnetic fields are generally considered harmful to living organisms. Designing magnetic materials to achieve efficient construction of magnetically anisotropic hydrogels while maintaining the biocompatibility of the entire process is a topic of significant importance.

The high manufacturability of hydrogel materials and the multifunctionality that can be imparted by magnetic anisotropy structures suggest their potential widespread applications in various biomedical fields, including tissue engineering, drug delivery, soft robotics, biosensing, magnetic hyperthermia, magnetic resonance imaging, bioseparation, *etc.*[38,46,55,121–124] On the path from magnetic anisotropic hydrogels in the laboratory to clinical use, many factors need to be considered, including mechanical properties, biocompatibility, *in vivo* safety, regulatory laws, and molecular mechanisms. We anticipate that this review, which focuses primarily on the prospects of magnetic anisotropic hydrogels in tissue engineering, may inspire more innovative studies and further advance the understanding, design, and application of magnetic fields, magnetic materials, and hydrogel materials.

Conflicts of interest

The authors declare no conflict of interest.

Acknowledgements

References

1 L. G. Griffith and M. A. Swartz, *Nat. Rev. Mol. Cell Biol.*, 2006, **7**, 211–224.

2 N. Khuu, S. Kheiri and E. Kumacheva, *Trends Chem.*, 2021, **3**, 1002–1026.

3 E. Prince and E. Kumacheva, *Nat. Rev. Mater.*, 2019, **4**, 99–115.

4 C. Frantz, K. M. Stewart and V. M. Weaver, *J. Cell Sci.*, 2010, **123**, 4195–4200.

5 B. S. Kim and D. J. Mooney, *Trends Biotechnol.*, 1998, **16**, 224–230.

6 Z. Zhao, R. Fang, Q. Rong and M. Liu, *Adv. Mater.*, 2017, **29**, 1703045.

7 W. Shi, J. Huang, R. Fang and M. Liu, *ACS Appl. Mater. Interfaces*, 2020, **12**, 5177–5194.

8 S. Landau, S. Ben-Shaul and S. Levenberg, *Adv. Sci.*, 2018, **5**, 1800506.

9 H. N. Kim, A. Jiao, N. S. Hwang, M. S. Kim, D. H. Kang, D. H. Kim and K. Y. Suh, *Adv. Drug Delivery Rev.*, 2013, **65**, 536–558.

10 R. L. Lieber and S. R. Ward, *Philos. Trans. R. Soc., B*, 2011, **366**, 1466–1476.

11 A. J. Sophia Fox, A. Bedi and S. A. Rodeo, *Sports Health*, 2009, **1**, 461–468.

12 S. R. Caliari and J. A. Burdick, *Nat. Methods*, 2016, **13**, 405–414.

13 Y. Li, J. Rodrigues and H. Tomas, *Chem. Soc. Rev.*, 2012, **41**, 2193–2221.

14 Y. S. Zhang and A. Khademhosseini, *Science*, 2017, **356**, eaaf3627.

15 H. L. Mao, S. J. Zhao, Y. X. He, M. Feng, L. H. Wu, Y. Y. He and Z. W. Gu, *Carbohydr. Polym.*, 2022, **285**, 119254.

16 K. Zhou, M. Feng, H. L. Mao and Z. W. Gu, *Biomater. Sci.*, 2022, **10**, 4479–4491.

17 W. Li, X. Yang, P. Lai and L. Shang, *Smart Med.*, 2022, **1**, e20220024.

18 Y. Piao, H. You, T. Xu, H.-P. Bei, I. Z. Piwko, Y. Y. Kwan and X. Zhao, *Eng. Regener.*, 2021, **2**, 47–56.

19 H. Wang, H. Zhang, Z. Xie, K. Chen, M. Ma, Y. Huang, M. Li, Z. Cai, P. Wang and H. Shen, *Eng. Regener.*, 2022, **3**, 407–419.

20 H. Zhang, D. Xu, Y. Zhang, M. Li and R. Chai, *Smart Med.*, 2022, **1**, e20220011.

21 A. Pardo, M. Gomez-Florit, S. Barbosa, P. Taboada, R. M. A. Domingues and M. E. Gomes, *ACS Nano*, 2021, **15**, 175–209.

22 J. C. Rose and L. De Laporte, *Adv. Healthcare Mater.*, 2018, **7**, 1701067.

23 Y. X. He, Y. Li, Y. D. Sun, S. J. Zhao, M. Feng, G. M. Xu, H. F. Zhu, P. H. Ji, H. L. Mao, Y. Y. He and Z. W. Gu, *Carbohydr. Polym.*, 2021, **261**, 117870.

24 L. Hao, S. Zhao, S. Hao, Y. He, M. Feng, K. Zhou, Y. He, J. Yang, H. Mao and Z. Gu, *Int. J. Biol. Macromol.*, 2023, **240**, 124364–124364.

25 C. E. Schmidt and J. B. Leach, *Annu. Rev. Biomed. Eng.*, 2003, **5**, 293–347.

26 G. Vunjak-Novakovic, N. Tandon, A. Godier, R. Maidhof, A. Marsano, T. P. Martens and M. Radisic, *Tissue Eng., Part B*, 2010, **16**, 169–187.

27 H. N. Kim, A. Jiao, N. S. Hwang, M. S. Kim, D. H. Kang, D.-H. Kim and K.-Y. Suh, *Adv. Drug Delivery Rev.*, 2013, **65**, 536–558.

28 K. J. De France, K. G. Yager, K. J. W. Chan, B. Corbett, E. D. Cranston and T. Hoare, *Nano Lett.*, 2017, **17**, 6487–6495.

29 L. Wang, G. Lu, Q. Lu and D. L. Kaplan, *ACS Biomater. Sci. Eng.*, 2018, **4**, 933–941.

30 M. T. I. Mredha, H. H. Le, T. Van Tron, P. Trtik, J. Cui and I. Jeon, *Mater. Horiz.*, 2019, **6**, 1504–1511.

31 Y. Wu, L. Wang, B. Guo and P. X. Ma, *ACS Nano*, 2017, **11**, 5646–5659.

32 R. F. Canadas, T. C. Ren, A. Tocchio, A. P. Marques, J. M. Oliveira, R. L. Reis and U. Demirci, *Biomaterials*, 2018, **181**, 402–414.

33 A. Gevorkian, S. M. Morozova, S. Kheiri, N. Khuu, H. Y. Chen, E. Young, N. Yan and E. Kumacheva, *Adv. Funct. Mater.*, 2021, **31**, 2010743.

34 K. K. Qin, C. Parisi and F. M. Fernandes, *J. Mater. Chem. B*, 2021, **9**, 889–907.

35 K. Sano, Y. Ishida and T. Aida, *Angew. Chem., Int. Ed.*, 2018, **57**, 2532–2543.

36 W. Chen, Z. Zhang and P. H. J. Kouwer, *Small*, 2022, **18**, e2203033.

37 J. C. Rose, M. Camara-Torres, K. Rahimi, J. Kohler, M. Moller and L. De Laporte, *Nano Lett.*, 2017, **17**, 3782–3791.

38 K. Hu, J. Sun, Z. Guo, P. Wang, Q. Chen, M. Ma and N. Gu, *Adv. Mater.*, 2015, **27**, 2507–2514.

39 K. Liu, L. Han, P. Tang, K. Yang, D. Gan, X. Wang, K. Wang, F. Ren, L. Fang, Y. Xu, Z. Lu and X. Lu, *Nano Lett.*, 2019, **19**, 8343–8356.

40 Q. Huang, Y. Zou, M. C. Arno, S. Chen, T. Wang, J. Gao, A. P. Dove and J. Du, *Chem. Soc. Rev.*, 2017, **46**, 6255–6275.

41 J. C. Rose, D. B. Gehlen, T. H. J. Koehler, C. J. Licht and L. De Laporte, *Biomaterials*, 2018, **163**, 128–141.

42 L. J. Santos, R. L. Reis and M. E. Gomes, *Trends Biotechnol.*, 2015, **33**, 471–479.

43 E. H. Fragal, V. H. Fragal, E. P. Silva, A. T. Paulino, E. C. da Silva, M. R. Mauricio, R. Silva, A. F. Rubira and E. C. Muniz, *Carbohydr. Polym.*, 2022, **292**, 119665.

44 S. Ganguly and S. Margel, *Prog. Polym. Sci.*, 2022, **131**, 101574.

45 Z. Li, Y. Li, C. Chen and Y. Cheng, *J. Controlled Release*, 2021, **335**, 541–556.

46 K. Li, J. Xu, P. Li and Y. Fan, *Composites, Part B*, 2022, **228**, 109401.

47 Z. Liu, J. Liu, X. Cui, X. Wang, L. Zhang and P. Tang, *Front. Chem.*, 2020, **8**, 124.

48 Y. Li, G. Huang, X. Zhang, B. Li, Y. Chen, T. Lu, T. J. Lu and F. Xu, *Adv. Funct. Mater.*, 2013, **23**, 660–672.

49 J. Cho and Y. Ishida, *Adv. Mater.*, 2017, **29**, 1605974.

50 L. Xue and J. Sun, *Front. Chem.*, 2022, **10**, 1040492.

51 N. A. Jalili, M. Muscarello and A. K. Gaharwar, *Bioeng. Transl. Med.*, 2016, **1**, 297–305.

52 E. A. Lee, H. Yim, J. Heo, H. Kim, G. Jung and N. S. Hwang, *Arch. Pharmacal Res.*, 2014, **37**, 120–128.

53 Y. Sahoo, M. Cheon, S. Wang, H. Luo, E. P. Furlani and P. N. Prasad, *J. Phys. Chem. B*, 2004, **108**, 3380–3383.

54 M. Antman-Passig and O. Shefi, *Nano Lett.*, 2016, **16**, 2567–2573.

55 R. Tognato, A. R. Armiento, V. Bonfrate, R. Levato, J. Malda, M. Alini, D. Eglin, G. Giancane and T. Serra, *Adv. Funct. Mater.*, 2018, **29**, 1804647.

56 S. Araújo-Custódio, M. Gomez-Florit, A. R. Tomás, B. B. Mendes, P. S. Babo, S. M. Mithieux, A. Weiss, R. M. A. Domingues, R. L. Reis and M. E. Gomes, *ACS Biomater. Sci. Eng.*, 2019, **5**, 1392–1404.

57 C. D. L. Johnson, D. Ganguly, J. M. Zuidema, T. J. Cardinal, A. M. Ziemba, K. R. Kearns, S. M. McCarthy, D. M. Thompson, G. Ramanath, D. A. Borca-Tasciuc, S. Dutz and R. J. Gilbert, *ACS Appl. Mater. Interfaces*, 2019, **11**, 356–372.

58 H. Chen, X. Zhang, L. Shang and Z. Su, *Adv. Sci.*, 2022, **9**, e2202173.

59 R. Goodrich, Y. Tai, Z. Ye, Y. Yin and J. Nam, *Adv. Funct. Mater.*, 2023, **33**, 2211288.

60 Z. Jiang, K. Shan, J. Song, J. Liu, S. Rajendran, A. Pugazhendhi, J. A. Jacob and B. Chen, *Life Sci.*, 2019, **220**, 156–161.

61 I. Khan, K. Saeed and I. Khan, *Arabian J. Chem.*, 2019, **12**, 908–931.

62 H. Markides, M. Rotherham and A. J. El Haj, *J. Nanomater.*, 2012, **2012**, 614094.

63 M. R. Sommer, R. M. Erb and A. R. Studart, *ACS Appl. Mater. Interfaces*, 2012, **4**, 5086–5091.

64 W. Liu, Y. Q. Li, S. Y. Feng, J. Ning, J. Y. Wang, M. L. Gou, H. J. Chen, F. Xu and Y. A. Du, *Lab Chip*, 2014, **14**, 2614–2625.

65 A. Omidinia-Anarkoli, S. Boesveld, U. Tuvshindorj, J. C. Rose, T. Haraszti and L. De Laporte, *Small*, 2017, **13**, 1702207.

66 X. Liu, B. Li, W. Wang, Y. Zhang, H. Li and Z. Li, *Chem. Eng. J.*, 2022, **449**, 137718.

67 K. Haraguchi and T. Takehisa, *Adv. Mater.*, 2002, **14**, 1120–1124.

68 T. Inadomi, S. Ikeda, Y. Okumura, H. Kikuchi and N. Miyamoto, *Macromol. Rapid Commun.*, 2014, **35**, 1741–1746.

69 E. Paineau, I. Dozov, I. Bihannic, C. Baravian, M.-E. M. Krapf, A.-M. Philippe, S. Rouziere, L. J. Michot and P. Davidson, *ACS Appl. Mater. Interfaces*, 2012, **4**, 4296–4301.

70 X. Lu, X. Feng, J. R. Werber, C. Chu, I. Zucker, J.-H. Kim, C. O. Osuji and M. Elimelech, *Proc. Natl. Acad. Sci. U. S. A.*, 2017, **114**, E9793–E9801.

71 L. L. Wu, M. Ohtani, M. Takata, A. Saeki, S. Seki, Y. Ishida and T. Aida, *ACS Nano*, 2014, **8**, 4640–4649.

72 M. Betsch, C. Cristian, Y. Y. Lin, A. Blaeser, J. Schoneberg, M. Vogt, E. M. Buhl, H. Fischer and D. F. D. Campos, *Adv. Healthcare Mater.*, 2018, **7**, e1800894.

73 L. Wang, T. Li, Z. Wang, J. Hou, S. Liu, Q. Yang, L. Yu, W. Guo, Y. Wang, B. Guo, W. Huang and Y. Wu, *Biomaterials*, 2022, **285**, 121537.

74 Y. Cao, P. X. Wang, F. D'Acierno, W. Y. Hamad, C. A. Michal and M. J. MacLachlan, *Adv. Mater.*, 2020, **32**, e1907376.

75 M. Liu, Y. Ishida, Y. Ebina, T. Sasaki, T. Hikima, M. Takata and T. Aida, *Nature*, 2015, **517**, 68–72.

76 C. N. Maganaris and J. P. Paul, *J. Physiol.*, 1999, **521**, 307–313.

77 S. Choi, Y. Choi and J. Kim, *Adv. Funct. Mater.*, 2019, **29**, 1904342.

78 D. Ye, P. Yang, X. Lei, D. Zhang, L. Li, C. Chang, P. Sun and L. Zhang, *Chem. Mater.*, 2018, **30**, 5175–5183.

79 G. Siqueira, D. Kokkinis, R. Libanori, M. K. Hausmann, A. S. Gladman, A. Neels, P. Tingaut, T. Zimmermann, J. A. Lewis and A. R. Studart, *Adv. Funct. Mater.*, 2017, **27**, 1604619.

80 B. Wang, J. G. Torres-Rendon, J. Yu, Y. Zhang and A. Walther, *ACS Appl. Mater. Interfaces*, 2015, **7**, 4595–4607.

81 M. Helminger, B. H. Wu, T. Kollmann, D. Benke, D. Schwahn, V. Pipich, D. Faivre, D. Zahn and H. Colfen, *Adv. Funct. Mater.*, 2014, **24**, 3187–3196.

82 E. Kasdorf, M. Engel and J. M. Perlman, *J. Pediatr. Neurol.*, 2013, **49**, 102–106.

83 C. Yu, C. F. Wang and S. Chen, *Adv. Funct. Mater.*, 2014, **24**, 1235–1242.

84 L. L. Hao, J. X. Li, P. Wang, Z. L. Wang, Z. X. Wu, Y. Wang, Z. X. Jiao, M. Guo, T. F. Shi, Q. G. Wang, Y. Ito, Y. Wei and P. B. Zhang, *Adv. Funct. Mater.*, 2021, **31**, 2009661.

85 L. Jiang, Y. Wang, Z. Liu, C. Ma, H. Yan, N. Xu, F. Gang, X. Wang, L. Zhao and X. Sun, *Tissue Eng., Part B*, 2019, **25**, 398–411.

86 J. Ramon-Azcon, S. Ahadian, M. Estili, X. Liang, S. Ostrovidov, H. Kaji, H. Shiku, M. Ramalingam, K. Nakajima, Y. Sakka, A. Khademhosseini and T. Matsue, *Adv. Mater.*, 2013, **25**, 4028–4034.

87 S. Ahadian, S. Yamada, J. Ramon-Azcon, M. Estili, X. Liang, K. Nakajima, H. Shiku, A. Khademhosseini and T. Matsue, *Acta Biomater.*, 2016, **31**, 134–143.

88 J. Ge, Y. Hu and Y. Yin, *Angew. Chem., Int. Ed.*, 2007, **46**, 7428–7431.

89 J. Ge and Y. Yin, *Adv. Mater.*, 2008, **20**, 3485–3491.

90 W. Luo, H. Ma, F. Mou, M. Zhu, J. Yan and J. Guan, *Adv. Mater.*, 2014, **26**, 1058–1064.

91 X.-Q. Wang, S. Yang, C.-F. Wang, L. Chen and S. Chen, *Macromol. Rapid Commun.*, 2016, **37**, 759–768.

92 L. L. Hao, J. X. Li, P. Wang, Z. L. Wang, Y. Wang, Y. Z. Zhu, M. Guo and P. B. Zhang, *Nanoscale*, 2023, **15**, 4123–4136.

93 L. L. Hao, L. L. Li, P. Wang, Z. L. Wang, X. C. Shi, M. Guo and P. B. Zhang, *Nanoscale*, 2019, **11**, 23423–23437.

94 A. M. Matos, A. I. Goncalves, A. J. El Haj and M. E. Gomes, *Nanoscale Adv.*, 2020, **2**, 140–148.

95 J. J. Zhuang, S. Y. Lin, L. Q. Dong, K. Cheng and W. J. Weng, *Acta Biomater.*, 2018, **71**, 49–60.

96 Y. Peng, Q.-J. Liu, T. He, K. Ye, X. Yao and J. Ding, *Biomaterials*, 2018, **178**, 467–480.

97 A. Tokarev, J. Yatvin, O. Trotsenko, J. Locklin and S. Minko, *Adv. Funct. Mater.*, 2016, **26**, 3761–3782.

98 M. C. Echave, R. M. A. Domingues, M. Gomez-Florit, J. L. Pedraz, R. L. Reis, G. Orive and M. E. Gomes, *ACS Appl. Mater. Interfaces*, 2019, **11**, 47771–47784.

99 C. Mueller, M. Trujillo-Miranda, M. Maier, D. E. Heath, A. J. O'Connor and S. Salehi, *Adv. Mater. Interfaces*, 2020, **8**, 2001167.

100 S. Jana, S. K. L. Levengood and M. Zhang, *Adv. Mater.*, 2016, **28**, 10588–10612.

101 T. H. Qazi, D. J. Mooney, M. Pumberger, S. Geissler and G. N. Duda, *Biomaterials*, 2015, **53**, 502–521.

102 H. Kwon, M. Guasch, J. A. Nagy, S. B. Rutkove and B. Sanchez, *Sci. Rep.*, 2019, **9**, 3145.

103 A. R. Armiento, M. J. Stoddart, M. Alini and D. Eglin, *Acta Biomater.*, 2018, **65**, 1–20.

104 A. Changoor, M. Nelea, S. Methot, N. Tran-Khanh, A. Chevrier, A. Restrepo, M. S. Shive, C. D. Hoemann and M. D. Buschmann, *Osteoarthritis Cartilage*, 2011, **19**, 1458–1468.

105 J. Malda, K. E. M. Benders, T. J. Klein, J. C. de Grauw, M. J. L. Kik, D. W. Hutmacher, D. B. F. Saris, P. R. van Weeren and W. J. A. Dhert, *Osteoarthritis Cartilage*, 2012, **20**, 1147–1151.

106 X. Yu, Z. Deng, H. Li, Y. Ma, X. Ma and Q. Zheng, *RSC Adv.*, 2022, **12**, 28254–28263.

107 R. Fuhrer, S. Hofmann, N. Hild, J. R. Vetsch, I. K. Herrmann, R. N. Grass and W. J. Stark, *PLoS One*, 2013, **8**, e81362.

108 J. Simińska-Stanny, M. Nizioł, P. Szymczyk-Ziółkowska, M. Brożyna, A. Junka, A. Shavandi and D. Podstawczyk, *Addit. Manuf.*, 2022, **49**, 102506.

109 E. Gracey, A. Burssens, I. Cambre, G. Schett, R. Lories, I. B. McInnes, H. Asahara and D. Elewaut, *Nat. Rev. Rheumatol.*, 2020, **16**, 193–207.

110 C. T. Thorpe and H. R. C. Screen, in *Metabolic Influences on Risk for Tendon Disorders*, ed. P. W. Ackermann and D. A. Hart, Springer Cham, 2016, vol. 920, pp. 3–10.

111 H. A. Lynch, W. Johannessen, J. P. Wu, A. Jawa and D. M. Elliott, *J. Biomech. Eng.*, 2003, **125**, 726–731.

112 T. Pesqueira, R. Costa-Almeida, S. M. Mithieux, P. S. Babo, A. R. Franco, B. B. Mendes, R. M. A. Domingues, P. Freitas, R. L. Reis, M. E. Gomes and A. S. Weiss, *J. Mater. Chem. B*, 2018, **6**, 1066–1075.

113 A. L. Wright, L. Righelli, T. J. Broomhall, H. C. Lamont and A. J. El Haj, *Front. Bioeng. Biotechnol.*, 2022, **10**, 797437.

114 A. Rehfeld, M. Nylander and K. Karnov, *Compendium of Histology*, Springer International Publishing, 2017.

115 J. T. Kevenaar and C. C. Hoogenraad, *Front. Mol. Neurosci.*, 2015, **8**, 44.

116 N. D. Leipzig and M. S. Shoichet, *Biomaterials*, 2009, **30**, 6867–6878.

117 P. Madhusudanan, G. Raju and S. Shankarappa, *J. R. Soc., Interface*, 2020, **17**, 20190505.

118 K. A. Clark, K. H. Nuechterlein, R. F. Asarnow, L. S. Hamilton, O. R. Phillips, N. S. Hageman, R. P. Woods, J. R. Alger, A. W. Toga and K. L. Narr, *J. Psychiatr. Res.*, 2011, **45**, 980–988.

119 S. Babu, I. Chen, S. Vedaraman, J. Gerardo-Nava, C. Licht, Y. Kittel, T. Haraszti, J. Di Russo and L. De Laporte, *Adv. Funct. Mater.*, 2022, **32**, 2202468.

120 K. A. Tran, Y. Jin, J. Bouyer, B. J. DeOre, L. Suprewicz, A. Figel, H. Walens, I. Fischer and P. A. Galie, *Biomater. Sci.*, 2022, **10**, 2237–2247.

121 P. Monks, J. K. Wychowaniec, E. McKiernan, S. Clerkin, J. Crean, B. J. Rodriguez, E. G. Reynaud, A. Heise and D. F. Brougham, *Small*, 2021, **17**, 2004452.

122 S. L. Shang, P. Zhu, H. Z. Wang, Y. G. Li and S. Yang, *ACS Appl. Mater. Interfaces*, 2020, **12**, 50844–50851.

123 J. Z. Xue, M. N. Yao, G. Y. Wang, Z. K. Wang, L. Shen, Q. P. Liu and Y. Liu, *Adv. Opt. Mater.*, 2021, **9**, 2100116.

124 L. Yang, J. Q. Miao, G. Li, H. Ren, T. S. Zhang, D. Guo, Y. F. Tang, W. F. Shang and Y. J. Shen, *ACS Appl. Polym. Mater.*, 2022, **4**, 5431–5440.